UCSF
UC San Francisco Electronic Theses and Dissertations

Title
The Effects of Osteocyte-Intrinsic TGF-Beta Signaling in Alveolar Bone During Orthodontic Tooth Movement

Permalink
https://escholarship.org/uc/item/8279b77q

Author
Ngo, Albert

Publication Date
2023

Peer reviewed|Thesis/dissertation

eScholarship.org Powered by the California Digital Library
University of California

The Effects of Osteocyte-Intrinsic TGF-Beta Signaling in Alveolar Bone During Orthodontic Tooth Movement

by
Albert Ngo

THESIS
Submitted in partial satisfaction of the requirements for degree of
MASTER OF SCIENCE

in

Oral and Craniofacial Sciences

in the

GRADUATE DIVISION
of the
UNIVERSITY OF CALIFORNIA, SAN FRANCISCO

Approved:

DocuSigned by:
Christina Hong
CE6EAA6FBA31451...

Christina Hong
Chair

DocuSigned by:
Tamara Alliston
[illegible]499...

Tamara Alliston

DocuSigned by:
Alice Goodwin
C84D7533F9714EF...

Alice Goodwin

Committee Members

DEDICATION AND ACKNOWLEDGEMENTS

This study would not have been possible without the amazing support of my team. I would first like to thank my mentor and principal investigator, Dr. Christine Yeumin Hong for giving me the opportunity to work on this novel project. She has given so much of her time to walk me through each step along the process, as well as help problem-solve and provide direction when things would go awry. I'd also like to thank Dr. Tamara Alliston, who has also met with me regularly to provide feedback on the project and supply our lab with the knockout mice samples. Thank you for helping our team brainstorm solutions to problems and always providing ideas on ways to improve the power and strength of our study from a more analytical research standpoint.

Jinsook Suh has also been instrumental in teaching me how to perform mouse surgeries, setting up the cages, providing the surgical materials, and walking me through the statistical analysis. I would not have been able to produce a quality thesis without her research experience. Jasmine Faldu, thank you for being by my side while we figured out how to establish the orthodontic tooth movement surgical model. She has inspired me to be innovative and think outside the box to make things work. I would also like to thank Dr. Alice Goodwin for being on my committee and providing feedback during my annual thesis update presentations. Thank you also to Dr. Sumit Yadav for meeting with our team virtually and providing suggestions on our surgical mouse model and sending us different wires to try in our experiments.

I would like to thank the dental students who have also helped me push this project along: Greg Pavlos, Ryan Hatmaker, Miya Eberlain, Byron Zhao, and Ursi Eisinger. They have helped me with a multitude of tasks throughout the past three years, from spending long nights in the surgical room sedating mice to checking and feeding the mice daily after the surgeries, they have

been my hands, eyes, and ears in making sure that everything gets done in a timely manner. They have assisted with data collection as well as figure making, which helped save me time so that this thesis can be completed as efficiently as possible.

Lastly, I would like to thank my friends and family for supporting me emotionally throughout the years, cheering for me when things get tough, and listening to me practice my oral presentations!

ABSTRACT

The Effects of Osteocyte-Intrinsic TGF-β Signaling in Alveolar Bone During Orthodontic Tooth Movement

by

Albert Ngo

Orthodontics is a specialty of dentistry that focuses on the correction of malpositioned teeth and jaws through dentofacial orthopedics. Thus, a critical understanding of tooth movement, retention, and relapse is crucial for clinical practice and treatment advancements for our patients. The foundation of orthodontic tooth movement (OTM) and relapse must be studied at the cellular level, by examining the role of osteocytes, the key cell present in bone. Many studies have explored the mechanisms underlying OTM and relapse but have focused more on the roles of osteoclasts and osteoblasts. Recent studies are now investigating osteocytes and unveiled that these cells are integral in mechanical-sensing in bone. On the molecular level, one of the pathways that is warranting further investigation is TGF-ß signaling in osteocytes with respect to orthodontic tooth movement. Studies showing that osteocytes directly remodel their perilacunar/canalicular matrix suggest that TGF-ß controls bone quality through this remodeling as well. TGF-ß has also been shown to stimulate osteocytes to increase RANKL production, ultimately leading to osteoclastogenesis in long bones. The aim of this study was to determine the extent to which osteocyte-intrinsic TGF-ß signaling in alveolar bone affects orthodontic tooth movement rate and alveolar bone remodeling. We employed TβRIIocy-/- mice to examine the mechanism of TGF-β signaling in osteocytes. TβRIIocy-/- and control littermates underwent OTM for 14 days through a spring assembly mesializing the upper left first molar. MicroCT scanning was used to measure factors such as orthodontic tooth movement rate, bone volume,

bone mineral density, alveolar bone height, root length, and root volume. The goal of this project was to analyze osteocyte function during orthodontic tooth movement and understand its mechanism so that we can safely and efficiently move teeth while reducing dental relapse potential afterwards. Thus, we can spark future clinical applications in orthodontic treatment and efficiency.

TABLE OF CONTENTS

1. Introduction……..……...……1

1.1 Preface……...……1

1.2 Cellular Processes in Bone……...…….……1

1.3 Role of Osteocytes During Orthodontic Tooth Movement…….……2

1.4 Biology and Biomechanics of Orthodontic Tooth Movement……3

1.5 Role of TGF-β Signaling in Bone Biology…….……4

2. Hypotheses……...……7

3. Specific Aims……...……8

4. Materials and Methods…….……9

4.1 Overview……9

4.2 Funding……..……..10

4.3 Sample Size and Subjects…….……10

4.4 Sedation and Pain Control……...……12

4.5 Orthodontic Appliance Treatment……...13

4.6 MicroCT Protocol……14

4.7 MicroCT Analysis……15

4.7.1 Orientation……15

4.7.2 Linear Measurements……22

4.7.3 Volumetric Measurements……28

4.8 Statistical Analysis……...43

5. Results……44

5.1 OTM……44

5.2 Alveolar Bone Remodeling……..45

5.3 Root Length and Root Volume……46

5.4 Aim 3 Retention-Relapse Model……*48*

6. Discussion……..49

6.1 Clinical Implications……52

6.2 Limitations……...52

6.3 Future Directions……54

7. Conclusions……55

8. References……..56

LIST OF FIGURES

Figure 1: *Schematic representation of the sample groups and experimental timeline for Aim 1 and Aim 2……11*

Figure 2: *Schematic representation of the sample groups and experimental timeline for Aim 3……12*

Figure 3: *Occlusal view of the orthodontic appliance treatment by placing a NiTi spring from the maxillary left first molar to the central incisors……13*

Figure 4: *(A) Active spring placed intraorally with 0.008" SS ligature wire tied to the molar and incisors with bis-GMA resin bonded for reinforcement (B) Bis-GMA resin used to deactivate the spring force and serve as an orthodontic retainer (C) Appliances removed to allow for orthodontic relapse……14*

Figure 5: *OTM distance (μm) measurements for KO and WT experimental and control groups……44*

Figure 6: *BV/TV (%) measurements for KO and WT experimental and control groups……45*

Figure 7: *BMD (g/cm^3) measurements for KO and WT experimental and control groups……46*

Figure 8: *ABH loss (mm) measurements for KO and WT experimental and control groups……46*

Figure 9: *Root length (mm) measurements for KO and WT experimental and control groups……47*

Figure 10: *Root volume (mm^3) measurements for KO and WT experimental and control groups……47*

Figure 11: *OTM distances for the orthodontic tooth movement, retention, and relapse model groups……48*

LIST OF ABBREVIATIONS

ABH: alveolar bone height

BMD: bone mineral density

BV/TV: bone volume fraction

CEJ: cemento-enamel junction

CTRL: control mouse group

KO: knockout mouse line

M1: maxillary left first molar

M2: maxillary left second molar

OTM: orthodontic tooth movement

PDL: periodontal ligament

PLR: perilacunar/canalicular remodeling

RANKL: receptor activator of nuclear factor k-β ligand

RL: root length

ROI: region of interest

RV: root volume

TGF-β: transforming growth factor–beta

TBRII: TGF-β receptor II

WT: wildtype mouse

1. INTRODUCTION

1.1 Preface

Orthodontics is a specialty of dentistry that focuses on the correction of mal-positioned teeth and jaws through dentofacial orthopedics. Thus, a critical understanding of tooth movement, retention, and relapse is crucial for clinical practice and treatment advancements for our patients. The foundation of orthodontic tooth movement (OTM) and relapse must be studied at the cellular level, by examining the role of osteocytes. Many studies have explored the mechanisms underlying OTM and relapse but have focused more on the roles of osteoclasts and osteoblasts. Recent studies are now investigating the roles of osteocytes and unveiled that these cells are integral in mechanical sensing in bone [14]. Osteocytes regulate the differentiation of osteoblasts (bone-forming cells) and osteoclasts (bone-resorbing cells) during bone remodeling induced by mechanical loading [15]. Matsumoto et. al. confirmed that osteocyte-ablated mice were resistant to bone loss, indicating that osteocytes play a crucial role in bone remodeling as there was a significant inhibition of tooth movement. By studying different molecular factors, cell functions can be elucidated and can then be used for drug targeting and potential therapeutics in healthcare. In orthodontics specifically, this may ultimately yield developments of new, innovative approaches to control tooth movement outcomes.

1.2 Cellular Processes in Bone

In review, bone contains osteons (Haversian systems), which are composed of a central canal (Haversian canal) surrounded by lamellae of bone matrix. Within the lamellae, there exist the osteocytes housed in spaces called lacunae. The osteocytes communicate with other osteocytes and cells within the bone through a network of canaliculi. Osteoblasts that lay down new bone become encased in its own bone matrix and are transformed into osteocytes, the most

abundant cellular component in bone [5]. The osteoblasts become quiescent at the end of bone remodeling, and they form flattened lining cells on the bone surface until a new remodeling cycle is triggered [14]. One of the most common signaling pathways in bone is the Osteoprotegrin (OPG) and Receptor Activator of Nuclear Factor k-β Ligand (RANKL) pathway. RANKL is synthesized by osteocytes and osteoblasts and functions in osteoclastogenesis [12]. RANKL has been identified as the membrane factor for osteoclast differentiation as it binds to the RANK receptor that exists on pre-osteoclasts. This binding causes a signaling cascade for osteoclast activation and commitment [22]. The RANKL/RANK binding is crucial for the differentiation, function, and survival of osteoclasts, and is the initial step of bone remodeling. Osteoprotegerin (OPG), another osteoblastic cell-derived factor, interrupts the RANKL/RANK binding as a decoy receptor of RANKL, thereby inhibiting osteoclastogenesis and favoring bone formation.

In osteoblasts, the expression of RANKL is up-regulated in the presence of interleukin-1, tumor necrosis factor α, or vitamin D, whereas transforming growth factor ß (TGF-ß) or estrogens have an opposite effect [23]. Osteocytes can regulate the expression of RANKL in osteoblasts, thus further influencing osteoclastogenesis. In addition to RANKL, the osteocyte product sclerostin (encoded by the SOST gene) serves to antagonize the canonical wnt signaling pathway, which leads to a reduced osteoblast activity. Sclerostin is exclusively synthesized by osteocytes to inhibit osteoblastogenesis and increase osteoblast apoptosis. Therefore, sclerostin is also regarded as a key inhibitor that regulates bone formation [15].

1.3 Role of Osteocytes During Orthodontic Tooth Movement

In addition to regulating the activity of osteoclasts and osteoblasts, osteocytes also engage in perilacunar/canalicular remodeling (PLR), during which they directly resorb and deposit bone matrix surrounding their intricate lacuna-canalicular network [1]. It is now clear

that PLR is a homeostatic mechanism that helps to maintain mineral homeostasis and bony infrastructure. PLR is the way osteocytes coordinate and conduct bone remodeling. Bone formation and breakdown occurs simultaneously in a dynamic system. Osteocytes are not static in this sense, and thus are regulating these processes in concert. Through expression of various extracellular matrix proteins, the scale will tip between balanced and unbalanced PLR. On the balanced side, we will see normal PLR enzyme expression which leads to organized collagen, normal mineralization, and lacunocanalicular maintenance. On the unbalanced side, we will see reduced PLR enzyme expression, which leads to disorganized collagen, hypermineralization, lacunocanalicular degradation, and osteonecrosis.

Several functions have been proposed for osteocytes, but the most notable being its function as mechano-sensory cells to detect mechanical stimuli produced from the mechanical loading of bones, and they are regulators of osteoblast and osteoclast function during bone remodeling [7]. Osteocytes communicate with one another, with cells on the bone surface, and with cells in the bone marrow space through this highly organized network of cellular processes [8]. Osteocyte processes are connected to each other through gap junctions, allowing for intracellular communication [9].

1.4 Biology and Biomechanics of Orthodontic Tooth Movement

OTM itself is a dynamic process that is completed by a repeated process of alveolar bone remodeling by bone resorption and bone formation. During OTM, mechanical force is placed on a tooth so that it can be moved through the alveolar bone. These forces induce strain on the bone tissue surrounding the tooth, leading to cellular responses that result in bone tissue remodeling [6]. Bone resorption through osteoclasts is seen on the side of the tooth that receives the pressure, whereas new bone is deposited through osteoblasts on the side of the tooth that senses the

tension. There are many proposed mechanisms for OTM, but the most popular hypotheses for osteocyte response include stress-induced bone matrix deformation/microcrack formation and fluid-flow shear stress. According to the micro-damage theory, the application of orthodontic force to the tooth strains the alveolar bone, causing micro-damage on the side of the tooth under pressure. Microcracks are more prevalent on the pressure-side than on the tension-side of the tooth, and it has been suggested that microcracks represent the first damage induced by orthodontic force. Additionally, it has been suggested that microcracks cause cellular damage, likely to the osteocyte processes, thereby inducing apoptosis and bone remodeling [24]. According to the fluid flow theory, the lack of fluid shear stress on the osteocytes occurs on the pressure side of the tooth, because the fluid is driven from a region of high pressure to a region of low pressure. Thus, osteoclast recruitment and bone resorption are enhanced [2]. Conversely, on the tension side, the increased pulling force on the periodontal ligament is transferred to the bone. The resulting deformation drives the fluid flow shear stress on the network of osteocytes. This shear stress induces osteocyte activation, and osteocytes respond by producing signaling molecules that contribute to osteoblast recruitment [12].

1.5 Role of TGF-β Signaling in Bone Biology

Although many molecular signaling pathways have been elucidated by many previous studies, there has been minimal research conducted on TGF-ß with respect to OTM. The mechanisms controlling bone quality are not well understood, but we know that TGF-ß plays an important role in that process in skeletal long bones. Studies showing that osteocytes directly remodel their perilacunar/canalicular matrix suggest that TGF-ß controls bone quality through PLR as well. When TGF-ß binds to its receptor on an osteocyte, this causes upregulation of PLR enzymes like MMP and CatK. Dole et. al. used inhibitors and mice with an osteocyte-intrinsic

defect in TGF-ß signaling (TβRII$^{ocy-/-}$) to show that TGF-ß regulates PLR in a cell-intrinsic manner to control bone quality [4]. TGF-ß produced by bone forming osteoblasts is sequestered in the extracellular matrix in an inactive, latent form. When released upon osteoclastic resorption of the extracellular matrix, TGF-ß exerts pleiotropic effects on osteoblasts, osteoclasts, and their progenitors to coordinate bone remodeling [23].

TGF-ß is a complex molecule that is secreted by all three cell types: osteoclasts, osteoblasts, and osteocytes. It serves to regulate the differentiation and function of both osteoblasts and osteoclasts, thereby balancing bone formation and resorption. TGF-β binds two types of TGF-β receptors: type I and type II. TGF-β RII transphosphorylates TGF-β RI and phosphorylates receptor-regulated Smads (R-Smads), which then dissociate from the tetrameric receptor complex and translocate to the nucleus to regulate transcription of target genes (MMP, RANK, OPG, CatK) to induce proliferation and early differentiation of osteoprogenitor cells, as well as chemotaxis of osteoprogenitor cells [23].

When this active TGF-ß binds to its receptor on an osteocyte, the downstream effects are increased osteocyte expression of RANKL and PLR enzymes, leading to osteoclastogenesis. This leads to robust canalicular length and mature mineral density in long bones. TGF-ß itself regulates diverse cellular behaviors ranging from fate specification, lineage selection, and differentiation, to epithelial–mesenchymal transition, migration, proliferation, and apoptosis [17]. When TGF-ß binds to its receptor on an osteoblast cell, it represses Runx2 transcription to inhibit osteoblast differentiation. When TGF-ß binds to its receptor on an osteoclast cell, acts directly on bone marrow macrophages and promotes osteoclastogenesis [23].

The growth factor TGF-ß is involved in both the regulation of and cellular response to the physical microenvironment. It is essential to discern the current findings regarding the

mechanisms by which these cells integrate physical and biochemical cues so that we can identify and address remaining gaps that could ultimately improve bone health. We need to further elucidate the role of TGF-ß in mechanobiological signaling in bone at the tissue and cellular levels leading to cell differentiation in order to optimize OTM and reduce relapse potential. Our proposed study strives to further examine the mechanism of TGF-ß in osteocytes and connect its direct effects on orthodontic tooth movement and alveolar bone remodeling. By bridging this connection, we can have a greater understanding of osteocyte function and spark future clinical applications in orthodontic treatment and efficiency.

2. HYPOTHESES

Osteocyte-intrinsic TGF-β signaling regulates orthodontic tooth movement through alveolar bone remodeling and tooth movement rate.

Ha: A defect in TGF-β signaling would decrease orthodontic tooth movement in a mouse model.

H_0: A defect in TGF-β signaling would had no effect on orthodontic tooth movement in a mouse model.

3. SPECIFIC AIMS

Aim 1: Determine the extent to which TGF-β signaling in osteocytes affects the rate of orthodontic tooth movement.

Aim 2: Determine the extent to which TGF-β signaling in osteocytes affects alveolar bone remodeling (bone volume, bone mineral density, alveolar bone height), root length, and root volume.

Aim 3: Establish a baseline retention and relapse protocol in a mouse model.

4. MATERIALS AND METHODS

4.1 Overview

This study aimed to investigate the impact of TGF-β signaling in osteocytes on orthodontic tooth movement and alveolar bone remodeling. Mice underwent general anesthesia and were subjected to single-sided orthodontic treatment in the maxillary left quadrant of the oral cavity. Untreated mice that did not undergo OTM were used as the control group. In the experimental group, the maxillary left side had an orthodontic nickel titanium spring ligated and bonded from the first molar to both maxillary incisors. Treatment lasted 14 days, a time frame previously established to be effective in studying OTM [24]. A widely utilized mouse OTM model was mirrored for this study [3] [10] [18]. At the completion of the study the mice were humanely euthanized as per IACUC protocols, and tissue samples were harvested for analysis.

For Aim 3 regarding retention and relapse, 3M UNITEK bis-GMA composite resin was applied to the spring assembly to deactivate the orthodontic forces. After the 14 days of OTM, an additional 14 days of retention was applied, followed by 7 days of relapse by removing the entire intraoral appliance.

OTM can be studied in many different animal species, but mice were chosen because they are an economical model and genetic manipulation is relatively easily controlled compared to other species. Mice also have a natural dentition landscape with one maxillary incisor in each quadrant and 3 molars separated by a long span (approximately 7mm). This natural distribution of teeth and edentulous space allows for OTM to be mimicked as it would be in a human moving teeth in the mesial/distal direction.

4.2 Funding

Funding for this project was provided by the American Association of Orthodontics Foundation and the National Institutes of Health under the leadership of Dr. Christine Hong.

4.3 Sample Size and Subjects

A power analysis was performed using conservative assumptions and based on data from prior studies by our group and others. We used the mean and standard deviation according to the type of assay from previous studies as well as previously performed OTM studies for the power calculation. Most OTM studies performed on mice required a sample size of n = 6-9 to detect significant differences in the craniofacial skeleton [4] [3] [23]. For OTM *in vivo* studies, power analysis using G*Power 3.1 shows >80% probability in detecting a difference between genotypes and sex with a two-sided alpha level of 0.05 and a sample size of 9 mice, yielding an effect size of dz=1.3. Using fewer animals does not allow us to detect a difference that would be clinically relevant.

A transgenic mouse line with osteocyte-specific deletion of TGF-β receptor II ($TBRII^{ocy-/-}$) was used for our experimental group. We used the genotype with Dmp1-Cre promoters that are osteocyte cell specific in order to excite the gene of interest. Twelve-week old adult mice were used in this study. For Aim 1 and Aim 2, all mice were male, consisting of a knockout group ($TBRII^{ocy-/-}$) with genotype $Dmp1\text{-}Cre^{+/-};TBRII^{fl/fl}$ and a wildtype control group (CTRL) with genotype $Dmp1\text{-}Cre^{-/-};TBRII^{fl/fl}$. The mice were divided into 4 groups: WT CTRL, KO CTRL, WT OTM, and KO OTM. Group A had 10 WT CTRL mice, Group B had 6 KO CTRL mice, Group C had 10 WT OTM mice, and Group D had 10 KO OTM mice [Figure 1]. Control groups did not undergo OTM but underwent the same sedation and received the same post-surgical soft gel diets. The OTM group had an orthodontic appliance applied to the maxillary left

side only. All mice were euthanized at 14 days with CO_2 asphyxiation and cervical dislocation, and their maxillae were harvested, hemisected, and fixed in 10% buffered formalin solution for microCT analysis. The protocol was approved by the UCSF Animal Research Committee.

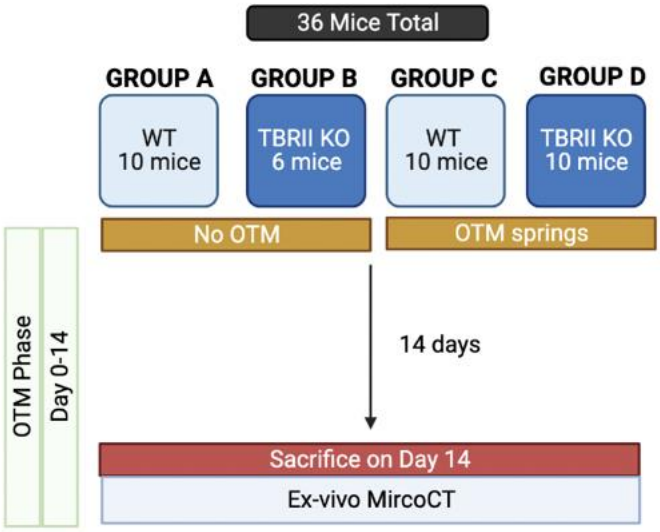

Figure 1: Schematic representation of the sample groups and experimental timeline for Aim 1 and Aim 2.

Aim 3 used 12-week old mice of mixed gender with heterozygous genotypes. There were 4 groups each with a sample size of 3. The smaller sample size was due to this aim being a pilot study that serves more as a "proof of concept" in determining if similar human retention/relapse trends can be reproduced in a mouse model. Group 0 was the OTM control group that underwent OTM for 28 days. Group 1 was the 14 day OTM group, Group 2 was the Retention group (14 days OTM followed by 14 days retention), and Group 3 was the Relapse group (14 days OTM, 14 days retention, followed by 7 days relapse). Sedation, OTM appliance assembly, diet, euthanasia, harvesting, and microCT imaging were done in the same way as Aim 1 and Aim 2.

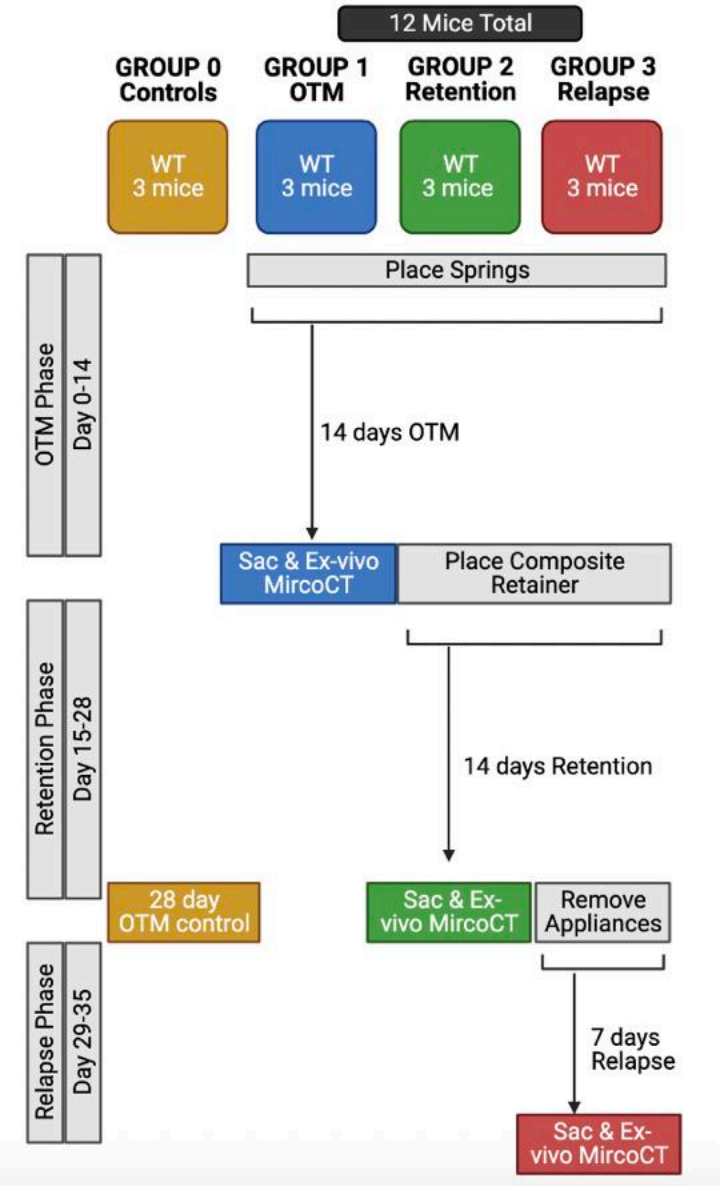

Figure 2: Schematic representation of the sample groups and experimental timeline for Aim 3.

4.4 Sedation and Pain Control

Prior to surgery and orthodontic appliance placement, mice were anesthetized by intraperitoneal injection of ketamine (87mg/kg) and xylazine (13mg/kg). 200uL Ketamine (100mg/mL) + 160uL Xylazine (20mg/mL) + 640uL Saline = 1 mL stored at 4C. 120-150uL of the 1 mL was used for IP injection per mouse (for adult mice 20g, anesthetized for 1.5-2 hours).

The mice were subsequently administered SR Buprenorphine (1.3 mg/mL) injected pre-operatively IP for analgesia.

4.5 Orthodontic Appliance Treatment

A handpiece was used to make retention grooves on the distal and facial surfaces of the maxillary incisors, 0.5mm from the gingival margin. A 0.008-inch stainless steel wire was threaded under the molar contact and adapted to encircle the maxillary first molar. A second ligature wire was tied similarly around both the maxillary central incisors. Additional stability was achieved by adding bis-GMA composite resin to the teeth and wires after self-etching primer (Transbond Plus, 3M Unitek, Monrovia, CA) was applied to the enamel. To minimize the movement of the maxillary left incisor, it was joined with the right incisor with the ligature wire and resin. The stainless-steel ligature wires were ligated to a low force/deflection rate nickel-titanium closed coil spring .010"x.030" delivering 5g of force at 2.5mm activation (Motion Dynamics Co) to deliver constant force for the protraction of maxillary first molar (Figure 3). For Aim 3, on Day 15, the mice were sedated and composite was applied to the spring system in order to deactivate the OTM spring force and serve as the "Retention Phase" (Figure 4). On Day 29, all appliances were removed under sedation and OTM was monitored for the remaining 7 days under the "Relapse Phase".

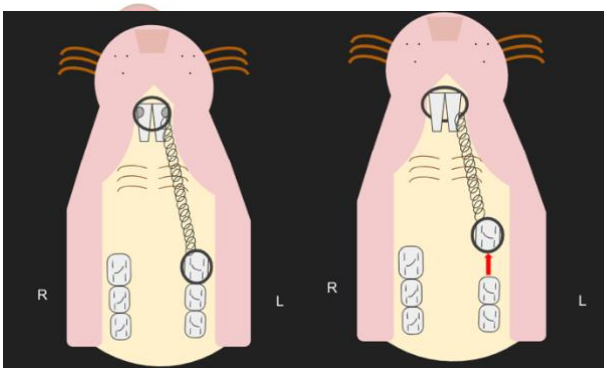

Figure 3: Occlusal view of the orthodontic appliance treatment by placing a NiTi spring from the maxillary left first molar to the central incisors.

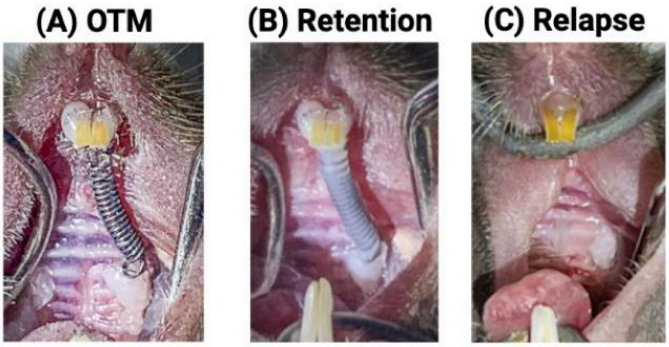

Figure 4: (A) Active spring placed intraorally with 0.008" SS ligature wire tied to the molar and incisors with bis-GMA resin bonded for reinforcement (B) Bis-GMA resin used to deactivate the spring force and serve as an orthodontic retainer (C) Appliances removed to allow for orthodontic relapse.

Following the spring placement, all sample mice were on a soft-food diet to avoid spring displacement. Mice were weighed and checked for appliance seating for the first 5 days, then every 3 days. Because mouse incisors erupt continuously, the appliances were monitored daily and incisors were trimmed as needed. Additional bonding material was added as needed. The mice were sacrificed on Day 14 (Aim 1 and Aim 2) or Day 35 (Aim 3).

4.6 MicroCT Protocol

For Aim 1 and Aim 2, mice in all groups underwent *ex-vivo* microCT imaging at Day 14. For Aim 3, mice underwent *ex-vivo* microCT imaging at Day 15, 29, and 35. Imaging was performed at the UCSF Core Center for Musculoskeletal Biology and Medicine (CCMBM) microCT core using Scanco MicroCT50 (Scanco Medical, Bruttisellen, Switzerland) for specimen imaging [43j]. For *ex-vivo* scanning, the skulls were scanned at an image resolution of 10 µm with 60kV using a 166-µA x-ray source and a 0.5mm aluminum filter. To ensure scan consistency, a calibration phantom of known geometry (a dense cylinder) was included for each of the scans.

4.7 MicroCT Analysis

OTM and relapse rate was determined by measuring the distance between the enamel at the heights of contour from the distal aspect of the first molar to the mesial aspect of the second molar (mircometers). This measurement was performed in both trans-axial and sagittal planes and compared to the measurements at the end of the retention phase for Aim 3. Bone volume and density was determined by measuring the bone mineral density (g/cm^3) and bone volume fraction (%). The ROI analyzed the bone volume of the furcation area of the maxillary first molar. Alveolar bone height (micrometers) was determined by measuring the bone height of the maxillary first molar at the level of the mesial root from the alveolar crest to the CEJ. Root length was determined by measuring the distance from the CEJ to the mesial root apex (micrometers). Root volume (mm^3) was determined by volumetric quantification of the mesial root of the maxillary left first molar.

After scanning the mice skulls and acquisition of the microCT data files, the images were reoriented on each 3-dimensional plane using Bruker Software DataViewer V1.5.6.2 to align the palate parallel to the trans-axial plane. We established a step-by-step protocol for each parameter of analysis:

4.7.1 Orientation

1. Obtain the Bruker Software DataViewer V1.5.6.2 and save the software the C:/ of the desktop.

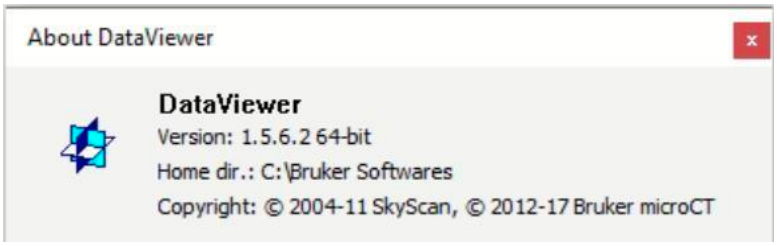

2. Select **Open Dataset.**

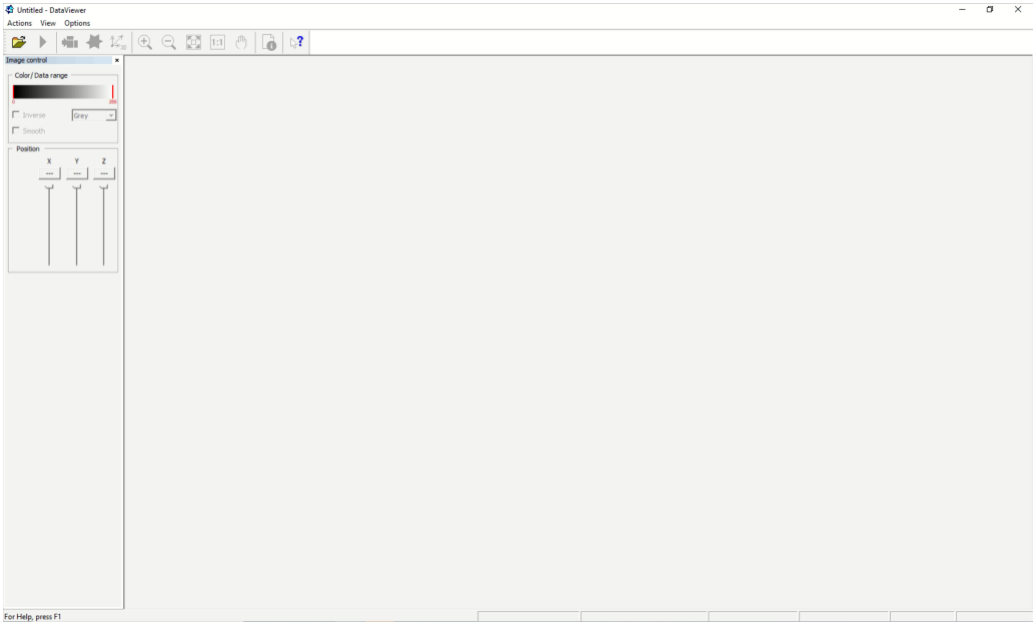

3. Open the folder for the scanned sample and select file types to view: **Dicom files (.dcm)**, then step two - double click on one image. DataViewer will automatically load all the pictures in its program.

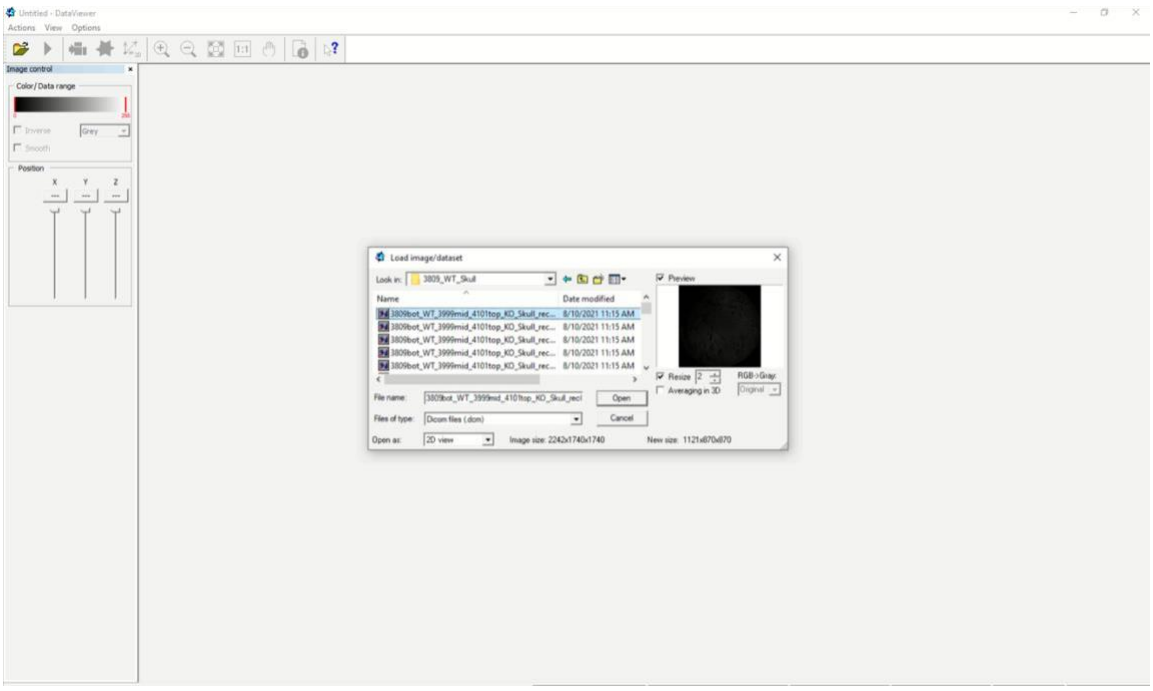

4. Click on **Load for 3D Viewing**

---

5. It will first check dataset integrity and then load images.

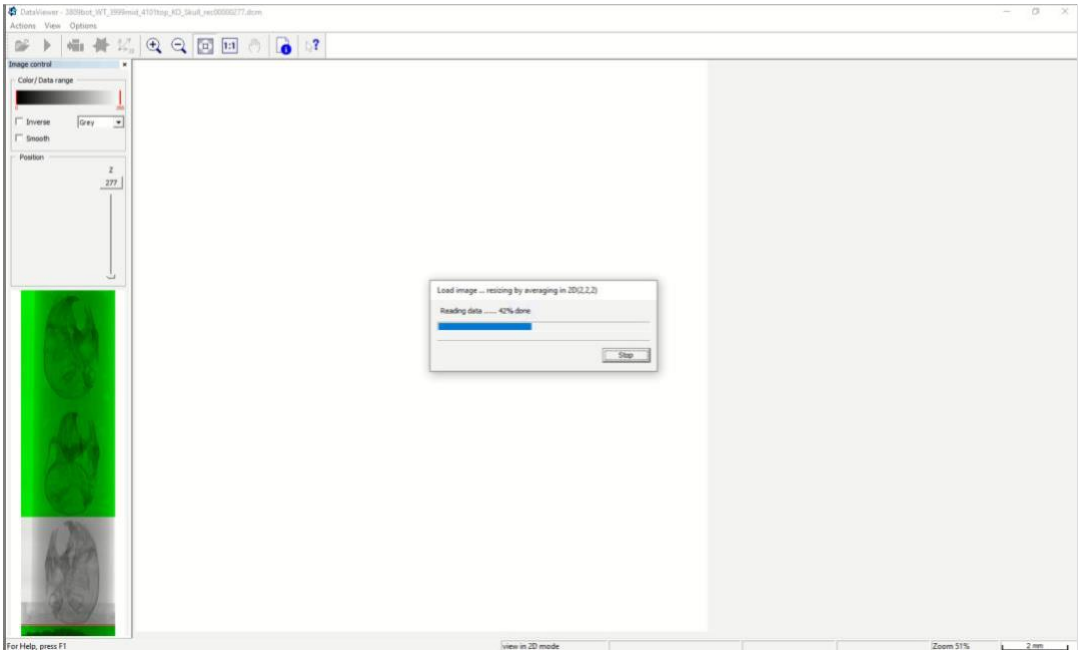

6. Right-click on mouse and control on the keyboard to manipulate the imaging in all three planes of space: level occlusal plane of molars horizontally, level palatal suture vertically, and align all three places of space to be perpendicular to each other. Press OK for “Attention!” popup.

7. Complete orientation in all three planes of space.

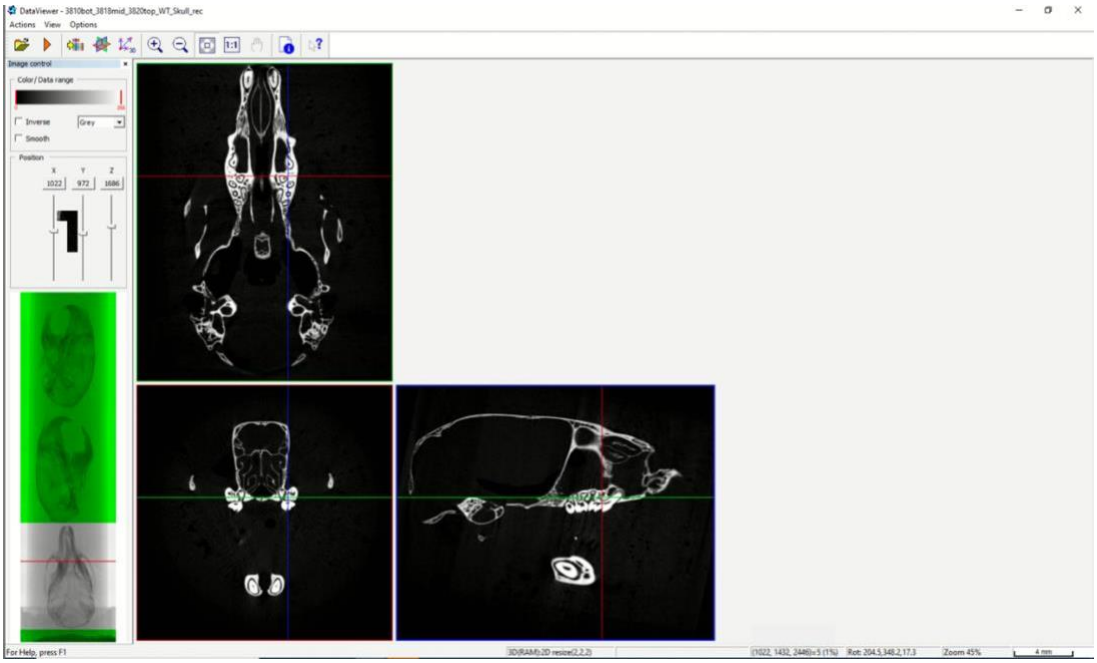

8. Once orientated properly, click **View** then **Single Volume of Interest.**

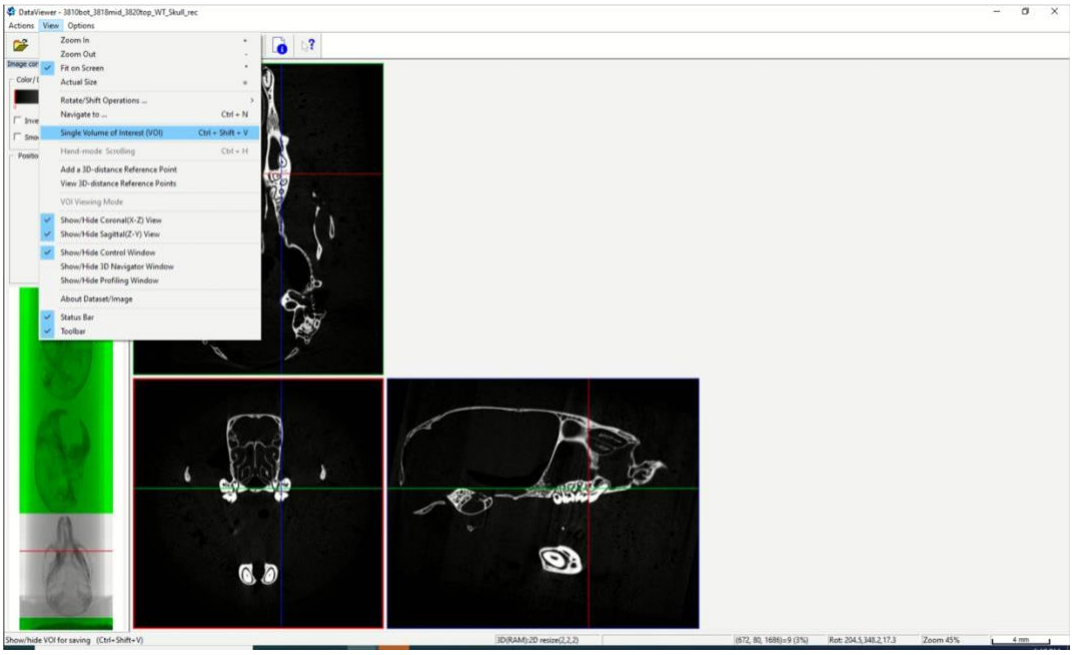

9. Manipulate the blue box that appears with right click on the mouse at the corners of the box to highlight the region of interest: maxillary left molars.

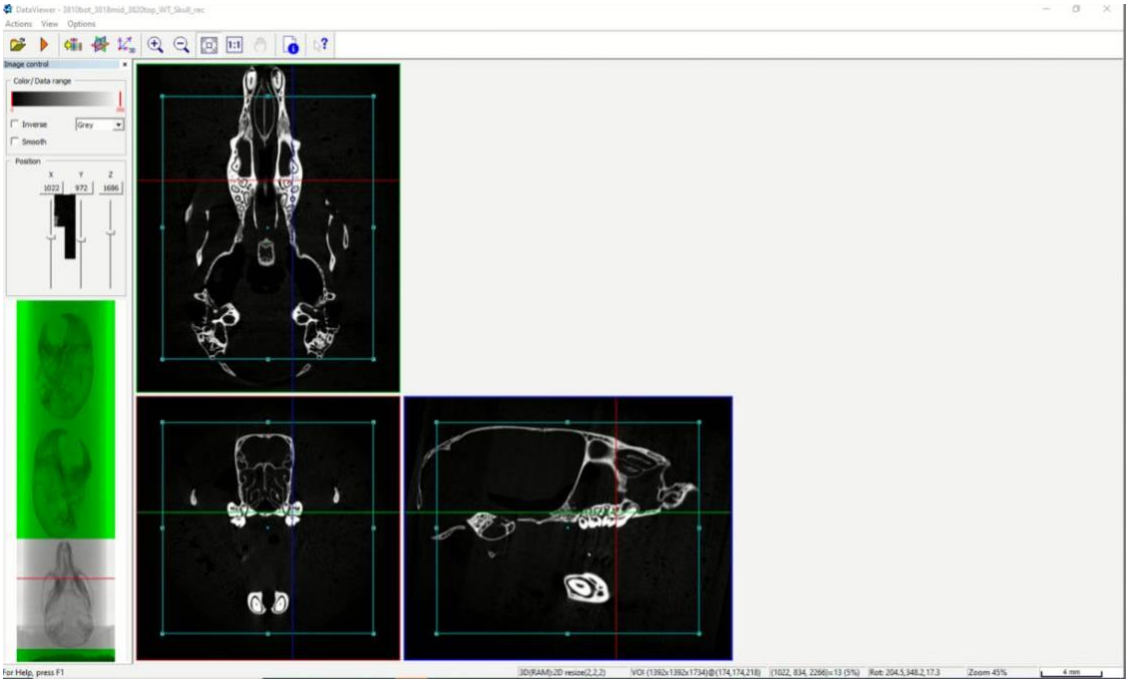

10. Once the selection for the volume of interest is done, click **Actions**.

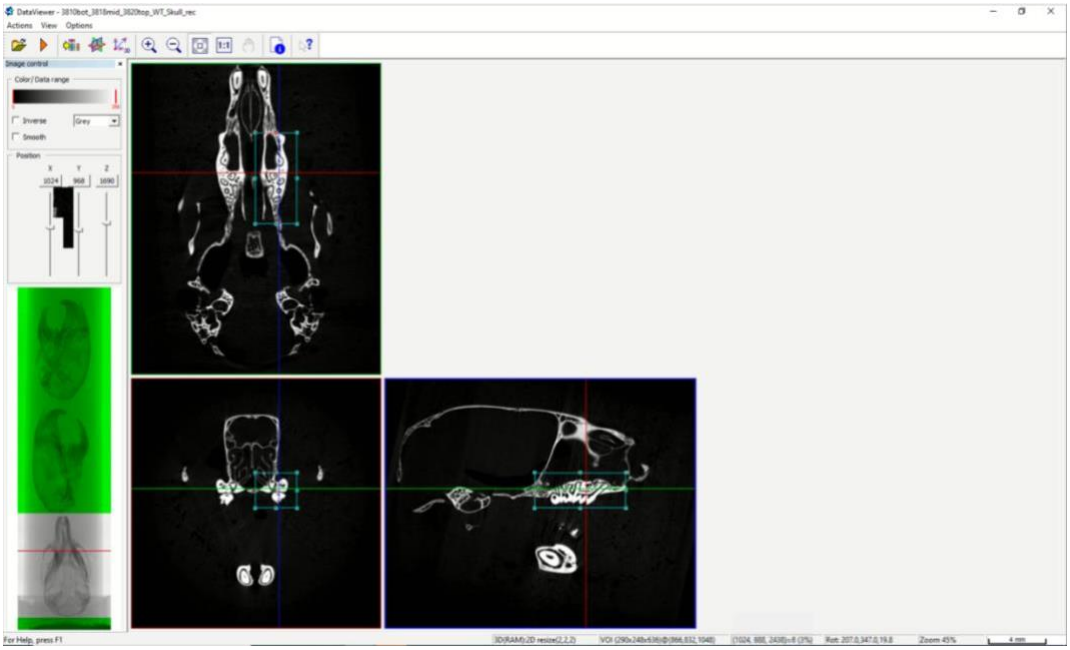

11. Click **Save…** and then **Select a VOI to Save…**

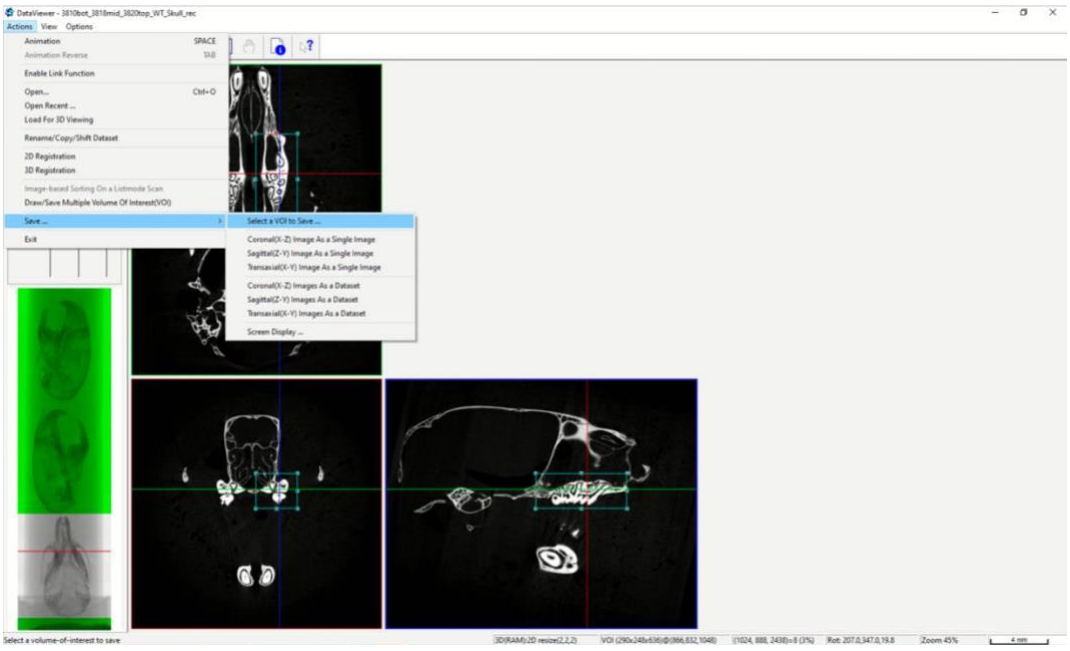

12. Pop-up dialogue “Options for saving a VOI” will appear. Select View to save: **Coronal (X-Z).**

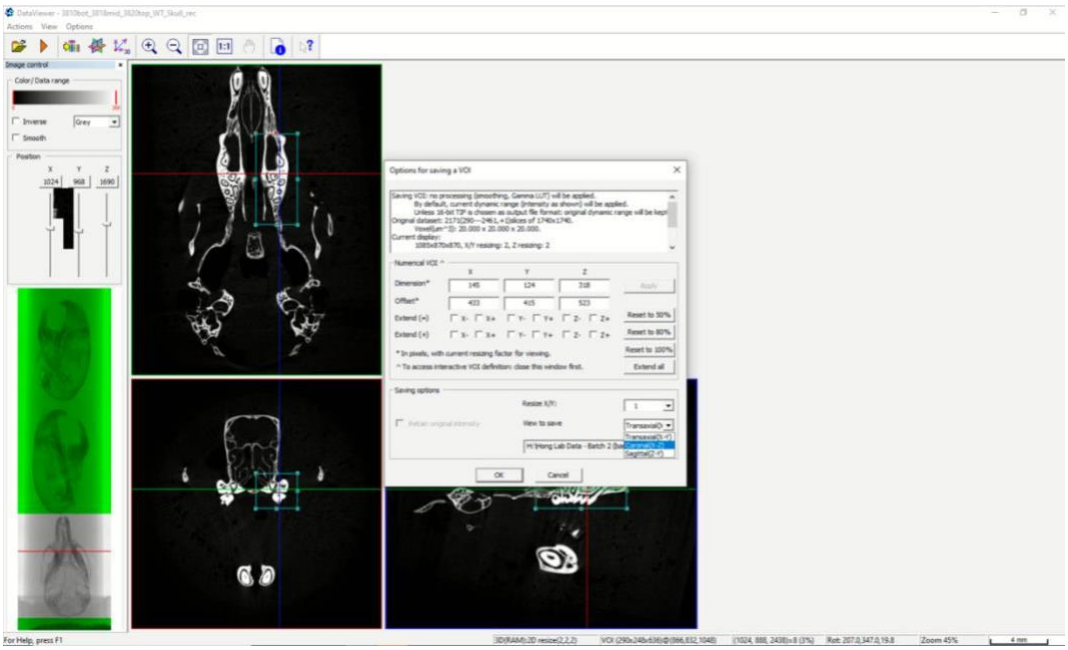

13. Select a destination folder for the new “region of interest” file to be saved by clicking “…”.

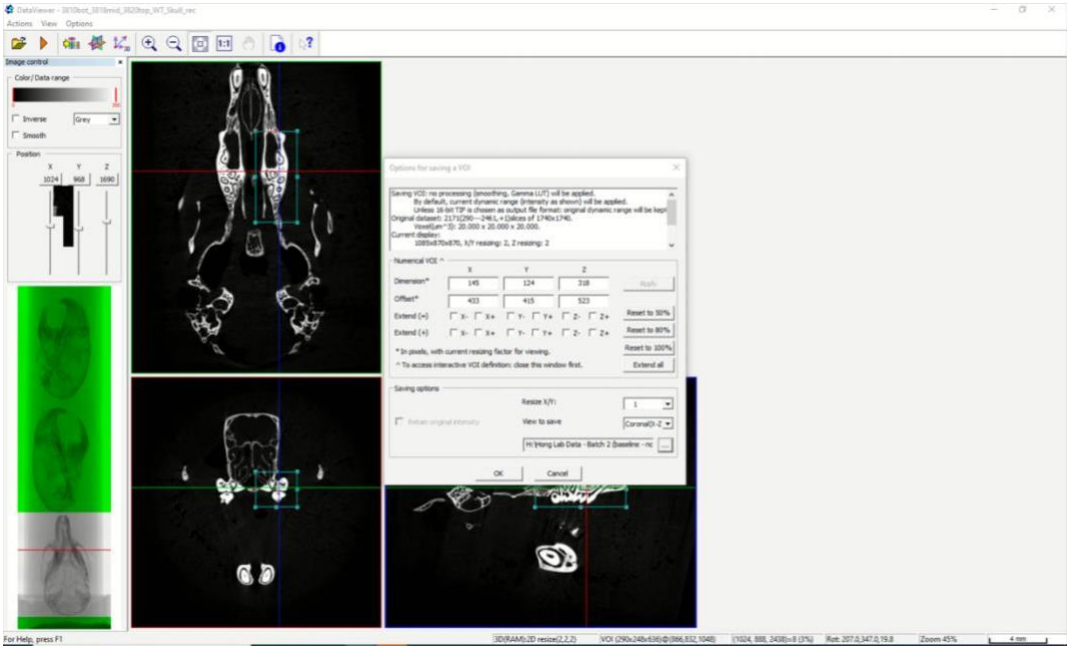

14. Now that the file is saved in the coronal view it can be opened in the 3D-Slicer software in order to analyze the linear tooth movement distance between the molars; it can also be opened in CTAn for volumetric analysis.

4.7.2 Linear Measurements

1. To measure OTM or relapse distance: Open 3D Slicer Software

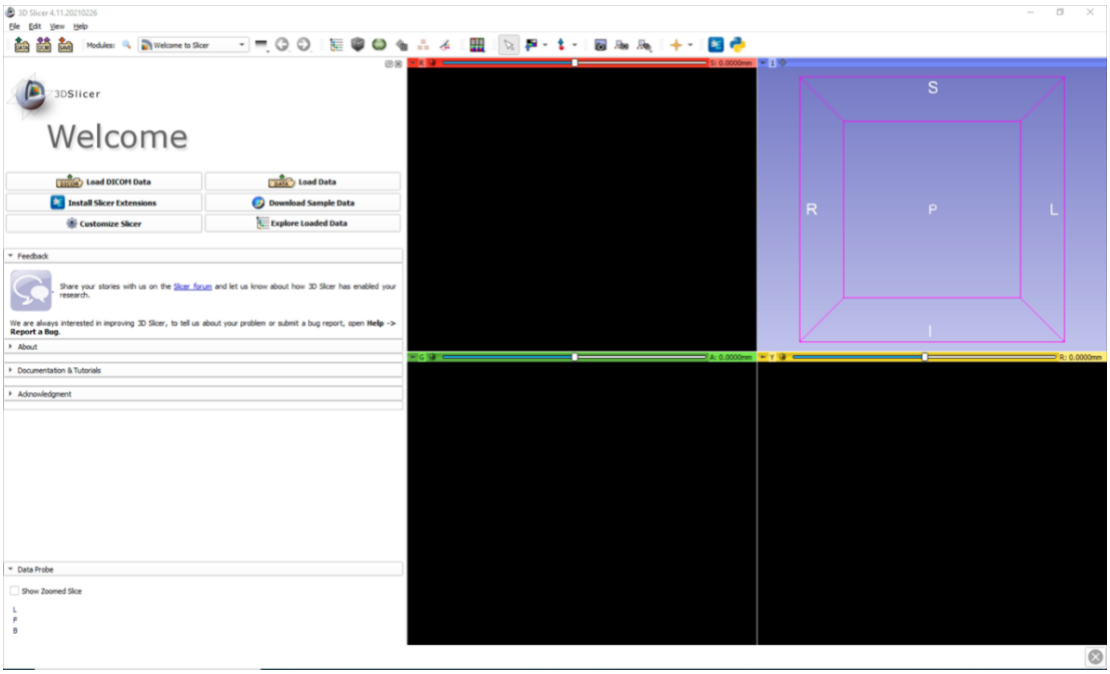

2. Select the drop down menu → SlicerMorph → Input and Output → ImageStacks

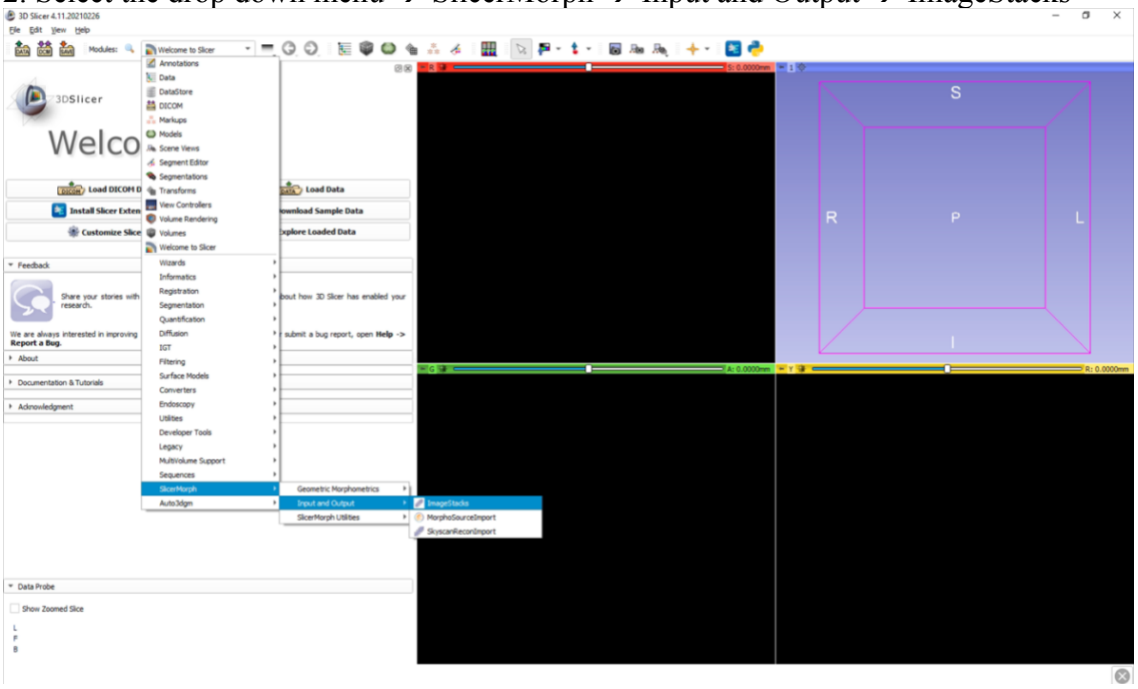

3. Select **Browse**… and double click on one file in the folder of interest

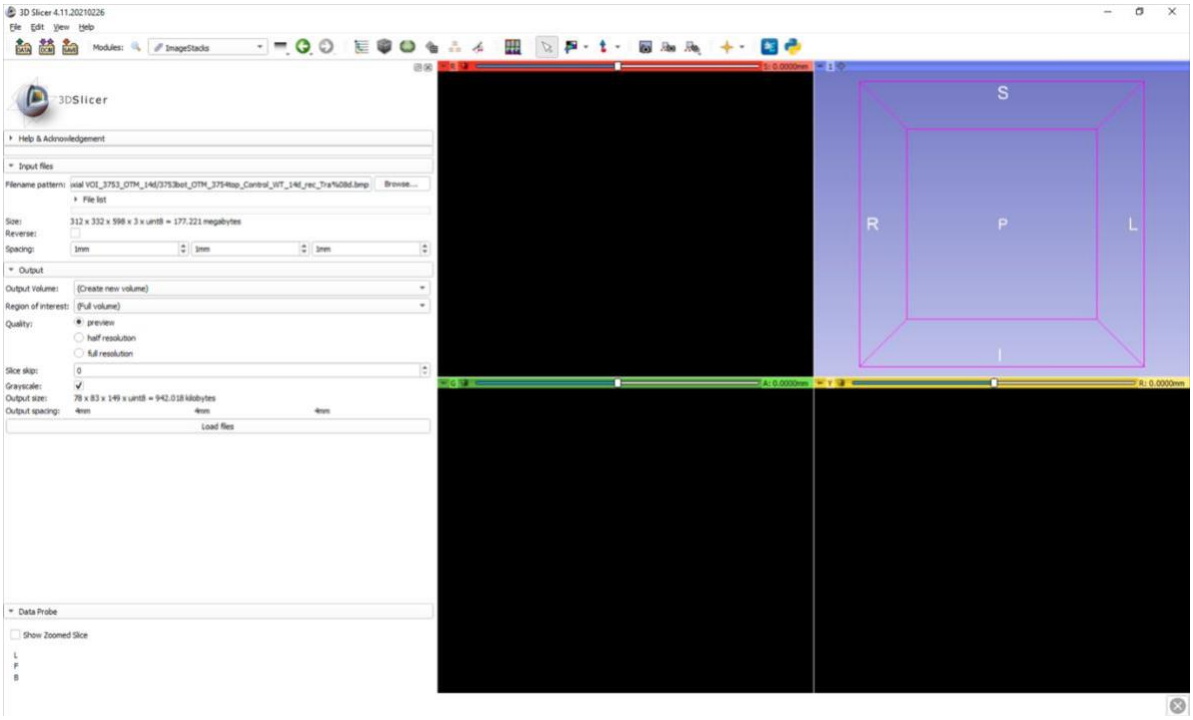

4. Change the spacing numbers to **0.01mm** in all three planes of space.

1. Output Volume: (Create new volume)
2. Region of interest: (Full volume)
3. Quality: full resolution

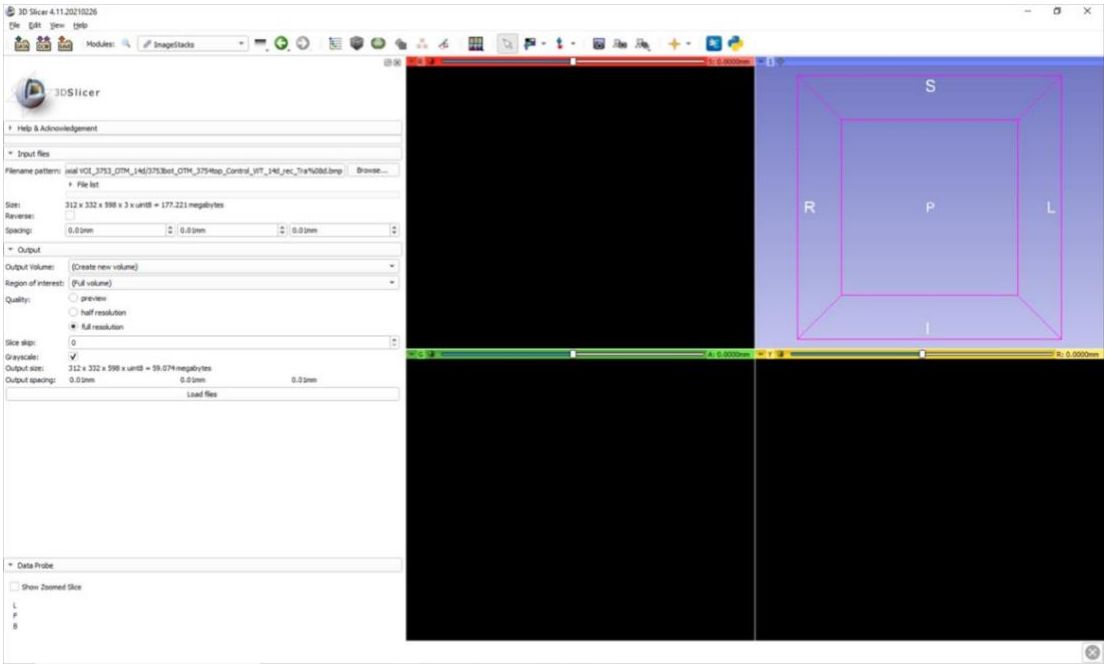

5. Once the microCT file deck is loaded, select **Volume Rendering** from the dropdown menu

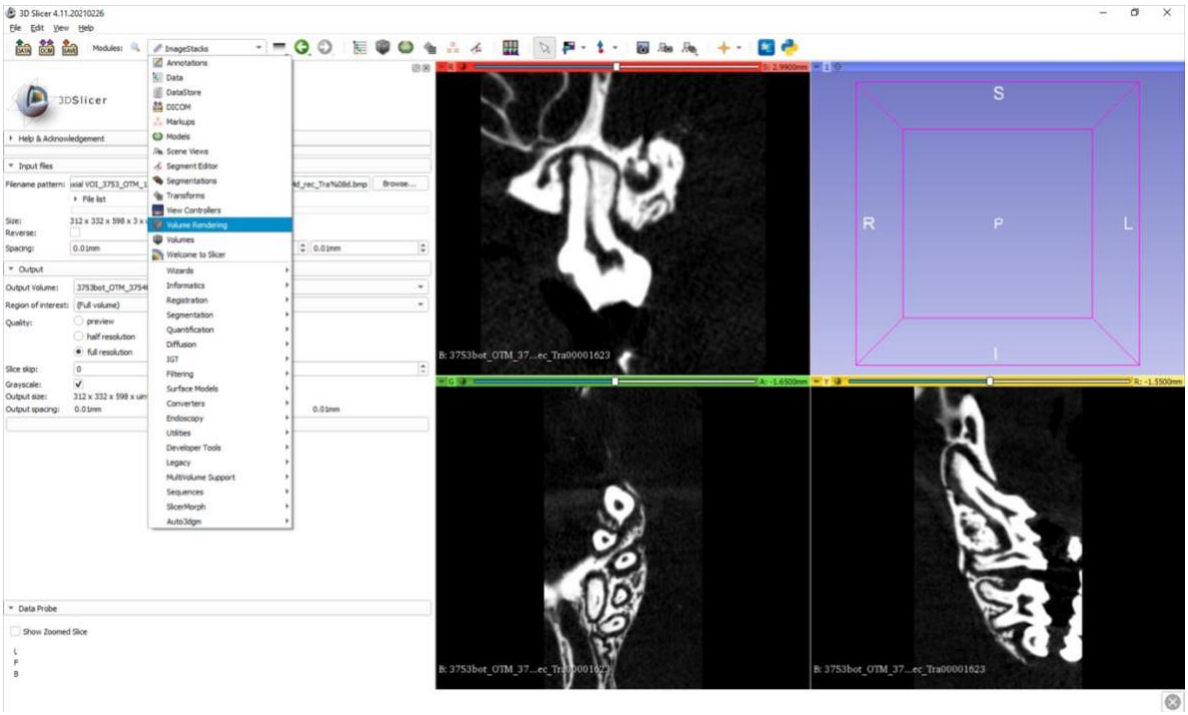

6. In the Display section, select preset: **CT-AAA**

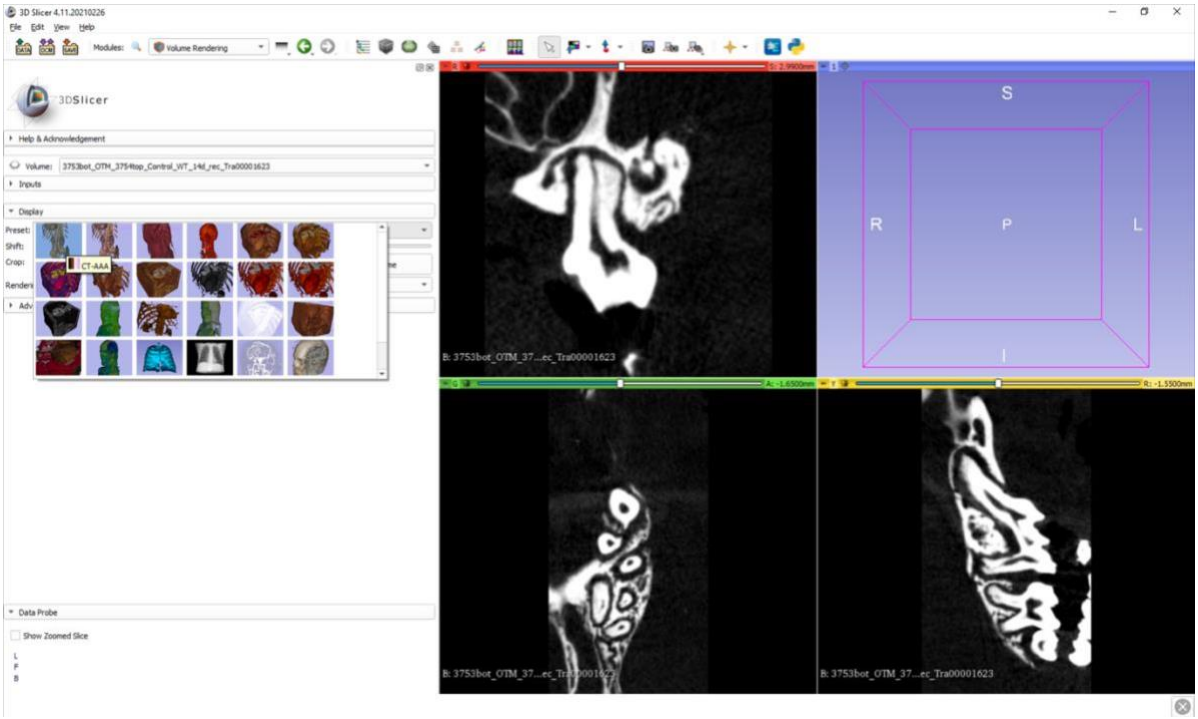

7. In the upper right box, the volume rendering will appear. Zoom in on the image until it is large enough to visualize clearly. Then, select **Markups.** Select this caption twice to create two markup points, one for each molar of interest.

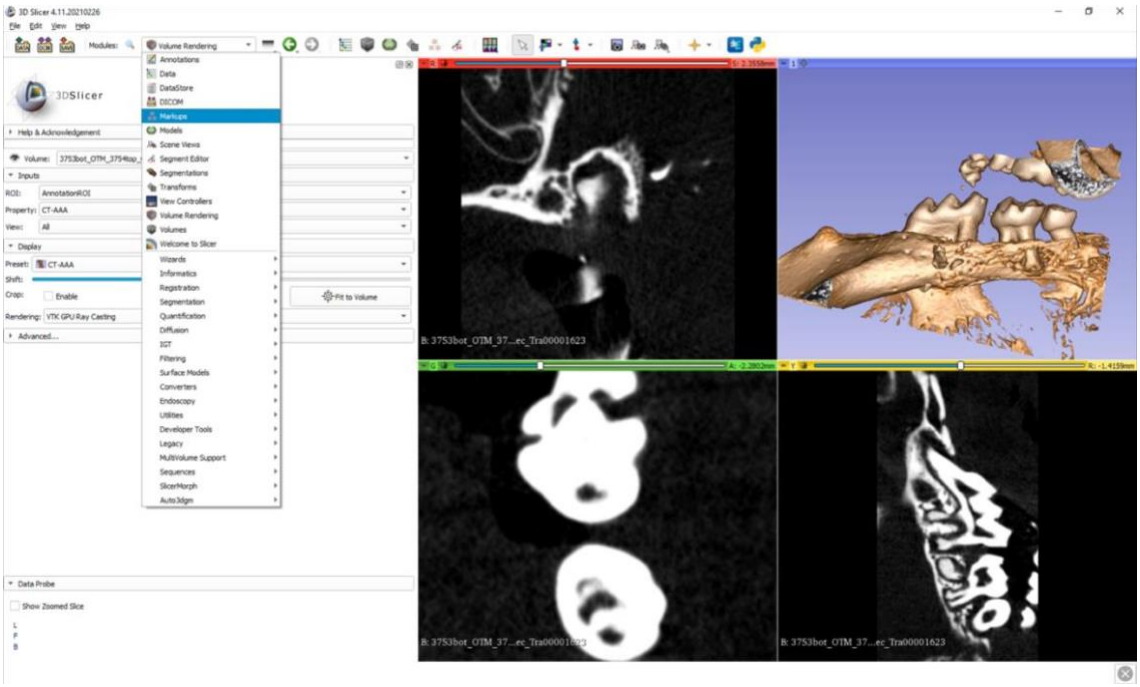

8. Left click on the mouse to rename the points **M1** and **M2**, which will represent the points for height of contour on the first molar and second molar.

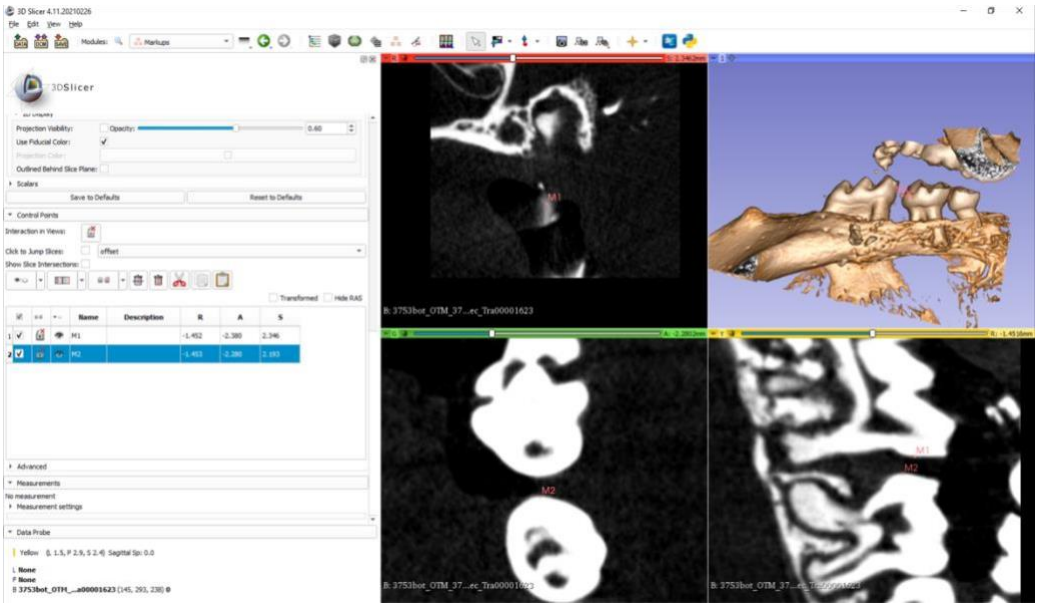

9. Use the scroll bars to move through the slices of the microCT in all three planes of space to find the height of contour on the first molar and second molar. Once located put the marker at that point desired. Record your points in a separate excel sheet to calculate the OTM distance as follows:

1. Summed linear distance: highlight both point M1 and M2, right click, summed linear distance measure = **c value**
2. Subtract the **"s value"** for M1 from the **"s value"** for M2 = **a value**
3. In excel calculate: **b value** =SQRT((c^2) - (a^2))

M1 to M2 distance (c value) (mm) (summed linear distance)	(a value) difference in s plane of space (mm)	b value (mm)

4. Excel:
5. **b value** * 1000 = ***distance of linear OTM in um***

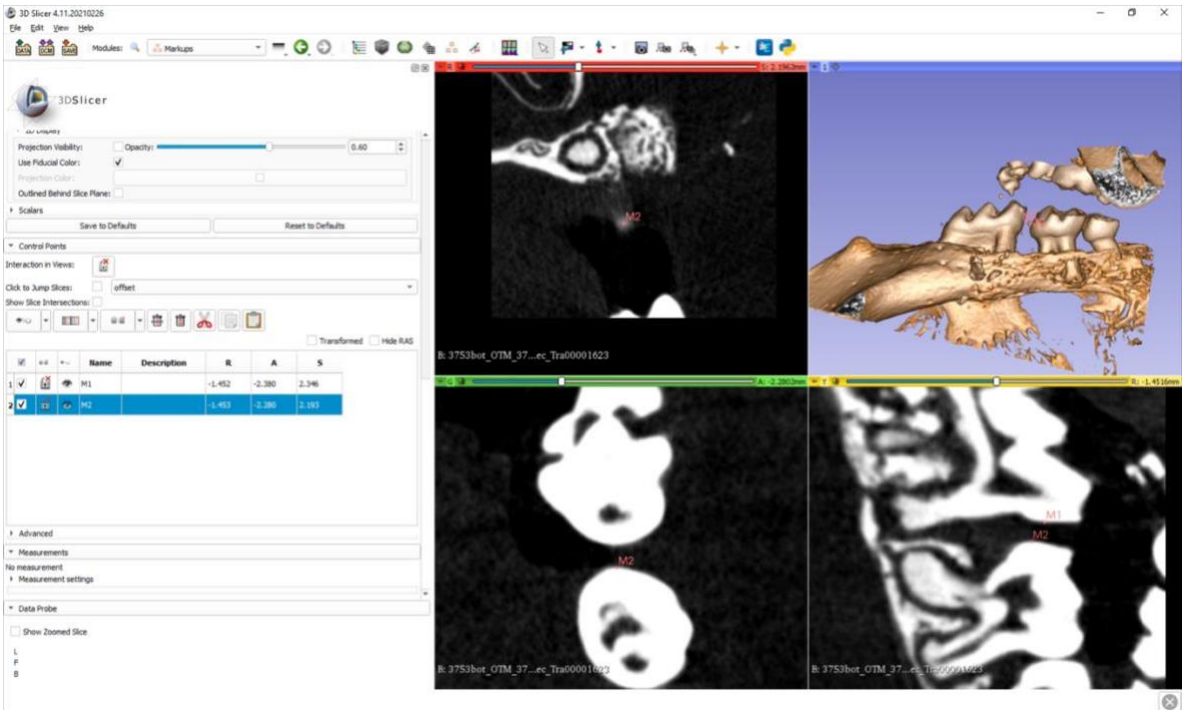

For measuring alveolar bone height (ABH), the 3D Slicer software was used again. ABH was measured at the mesial root of the maxillary left first molar. Using the software, we measured the distance from the cemento-enamel junction to the alveolar crest on the mesial side of the mesial-buccal root.

For measuring root length (RL), the 3D Slicer software was used again. RL was measured at the mesial root of the maxillary left first molar. Using the software, we measured the distance from the CEJ to the root apex of the mesial-buccal root.

1. Follow the 3D Slicer protocol above to open the file in all 3 planes of space and render the 3D volume
2. Set 3D image looking straight at the lingual of M1, the mesial on the left side, and the occlusal table horizontal

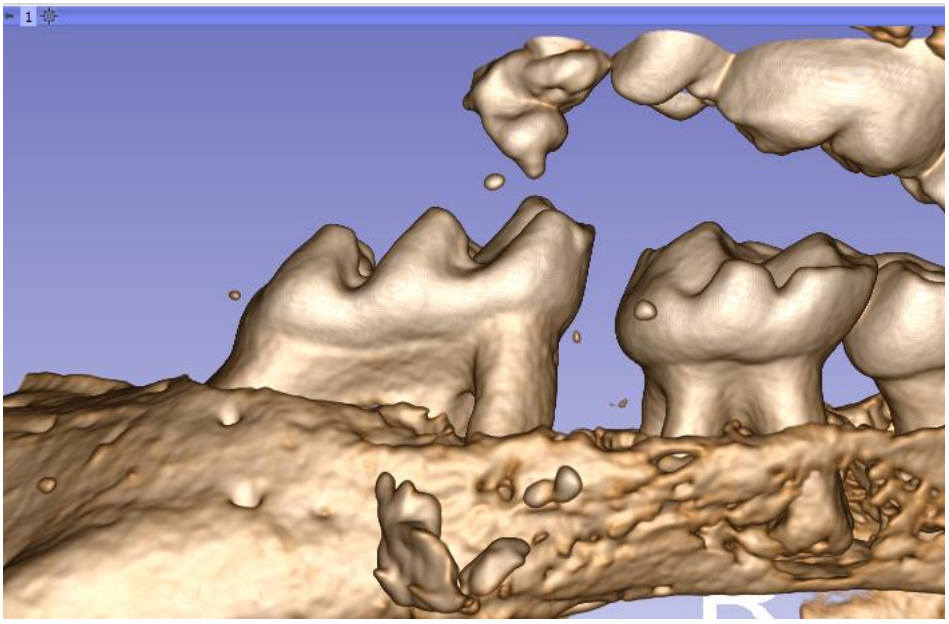

3. Hold shift key and hover mouse over the CEJ until you get to the mesial CEJ
    a. Record the CEJ value (A value) from the transverse view
4. Scroll down the transverse view until you see the first speck of mesial alveolar bone height
    a. Record the ABH value (A value)

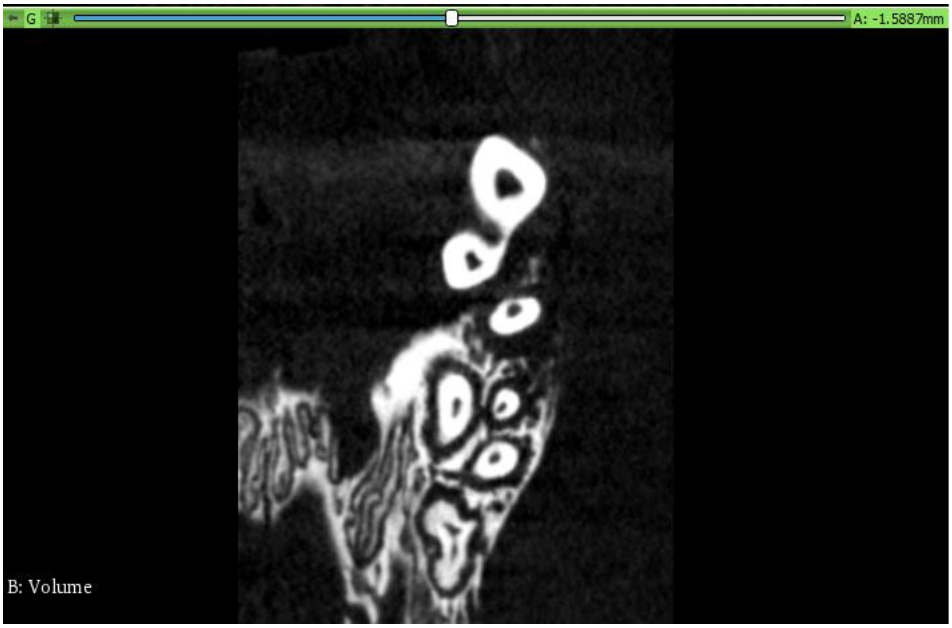

5. Scroll down the transverse view until you see the last slice with the mesial root apex→records the apex value (A value)
6. Subtract the CEJ A value from the ABH A value to get the ABH level loss
7. Subtract the CEJ A value from the RL A value to get the total root length

4.7.3 Volumetric Measurements

1. To measure BMD and BV/TV: Open the CTAn software and click on **open file.**

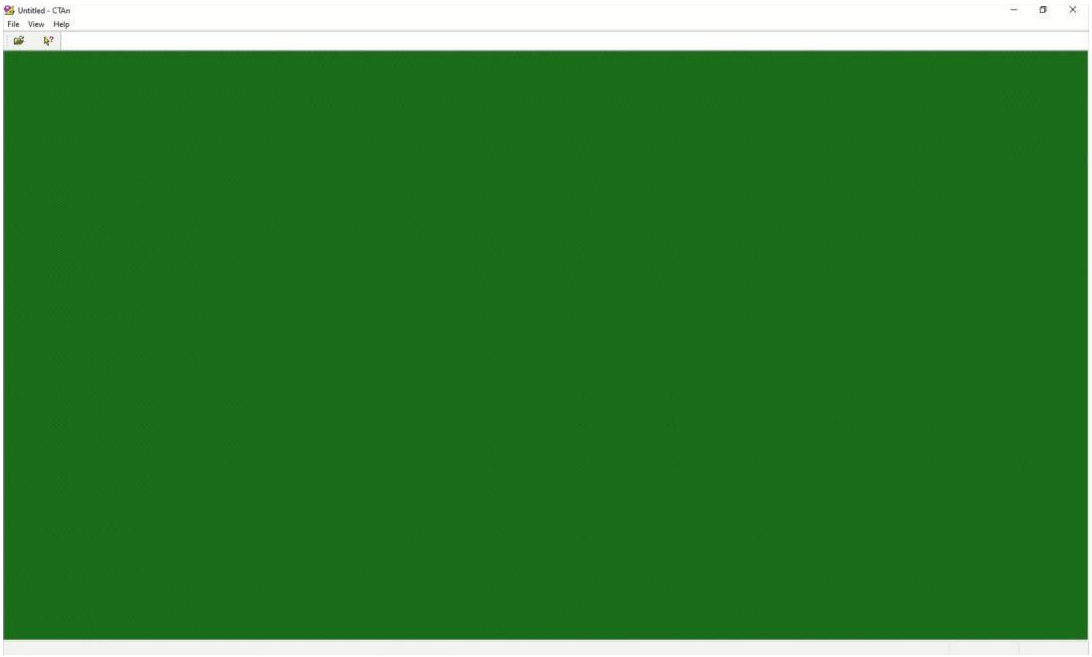

2. Find the file of interest and double click on the file to load. Select **open.**

3. Scroll through the files and find the slice that shows the first speck of bone for the furcation area.

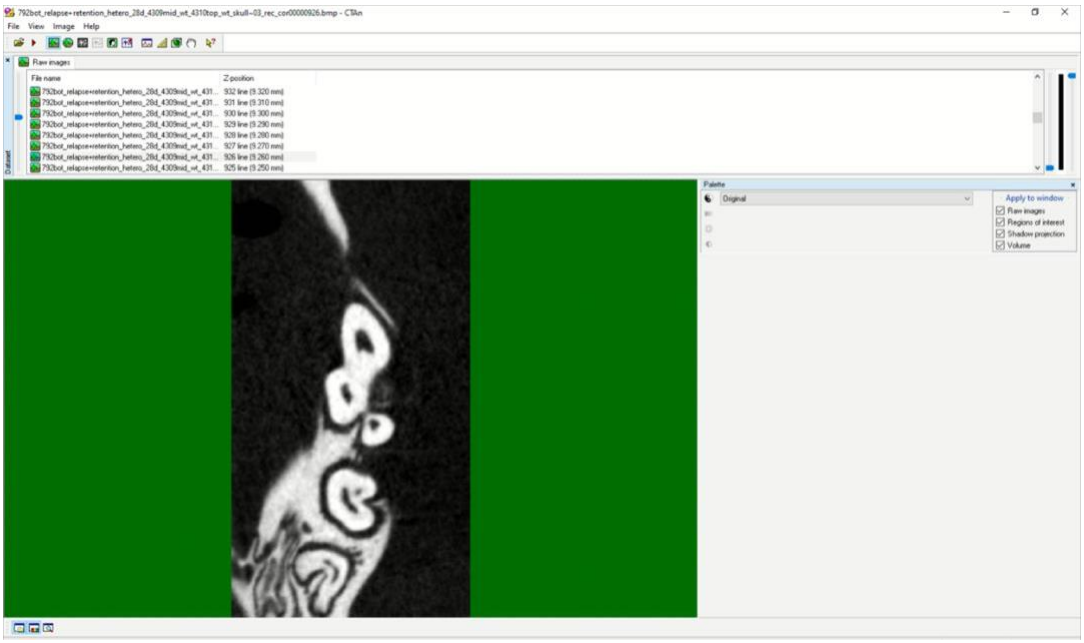

4. Use the file Z position and subtract 0.2mm to find the first slice for the region of interest. Right click on that slice and select Set the Top of Selection

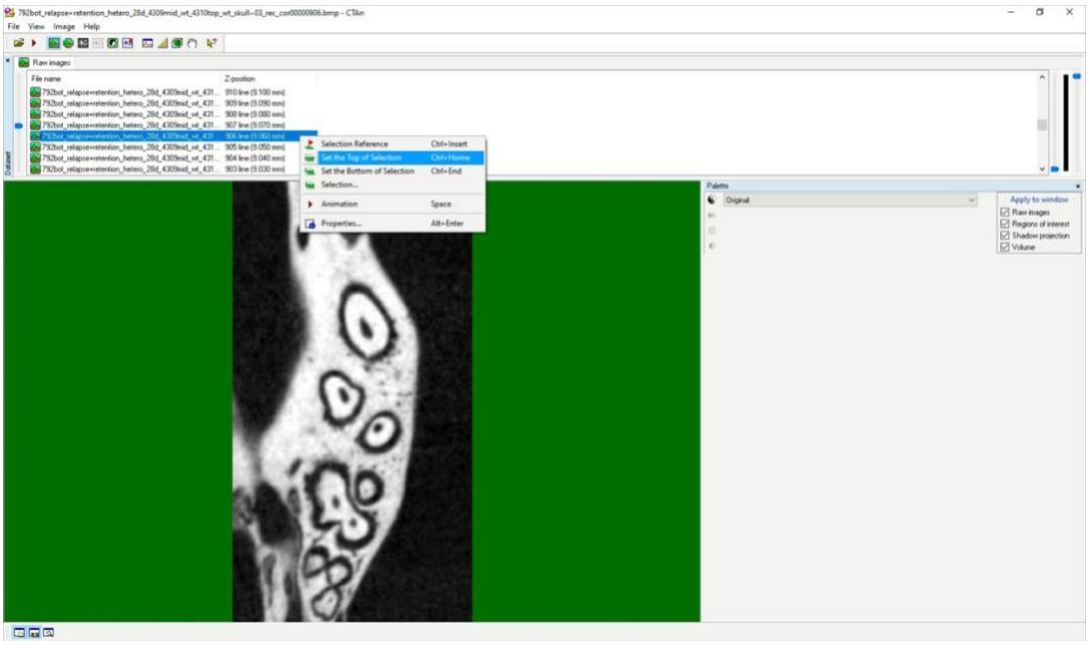

5. From the Top of Selection and subtract 0.35mm to find the slice for the region of interest. Right click on that slice and select Set the Bottom of Selection

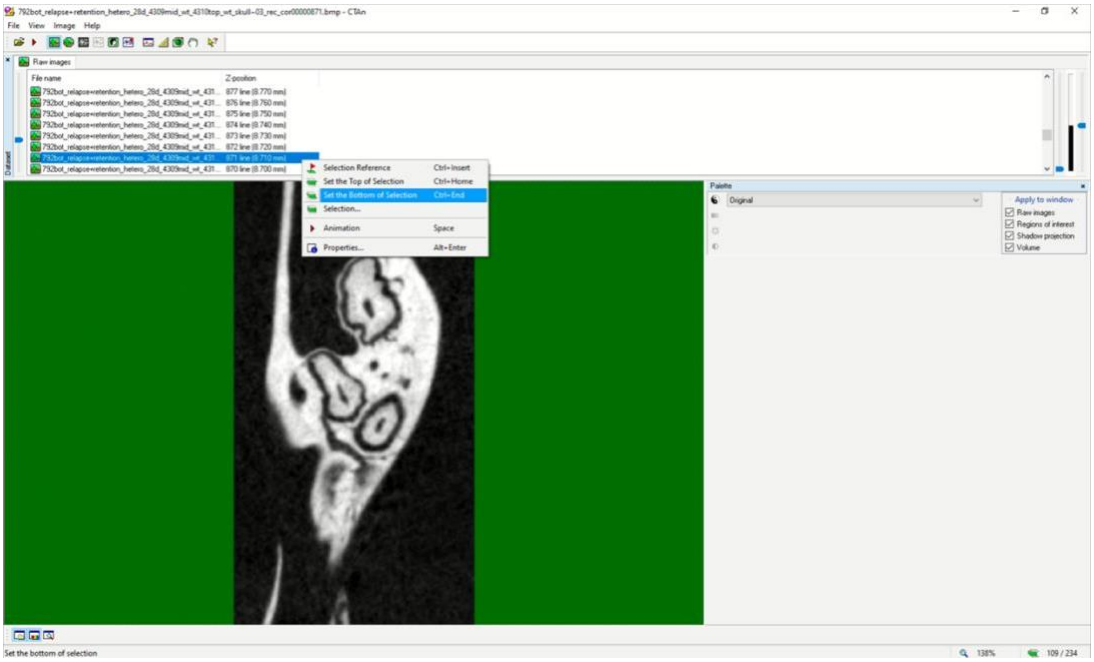

6. Now the top and bottom boundaries of the region of interest are selected

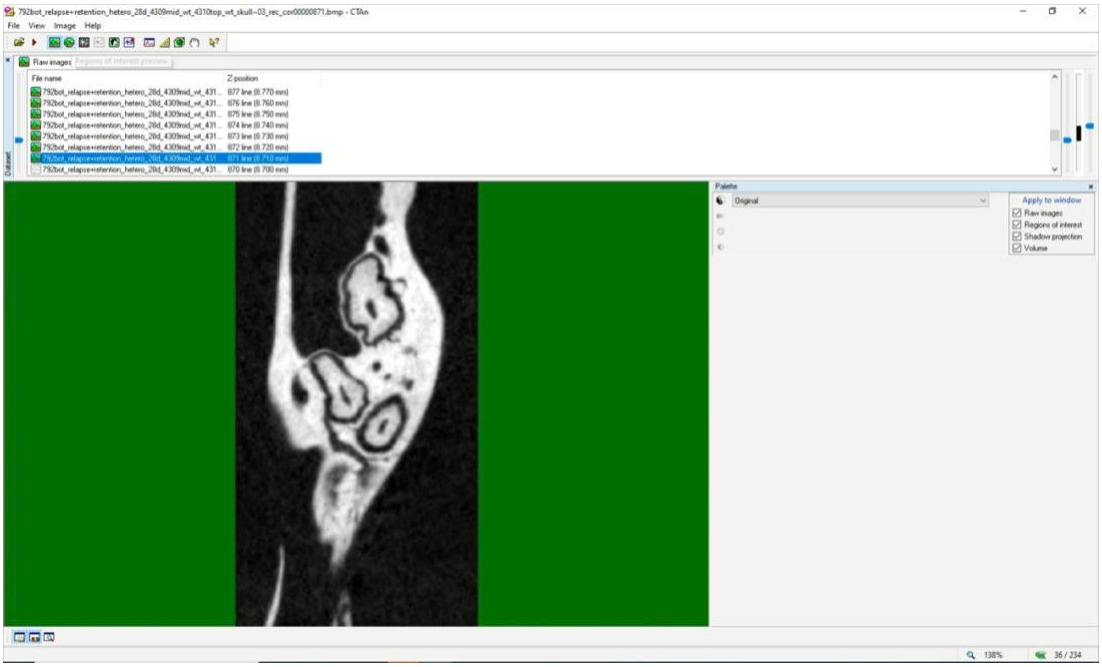

7. Select the next tab **regions of interest preview**

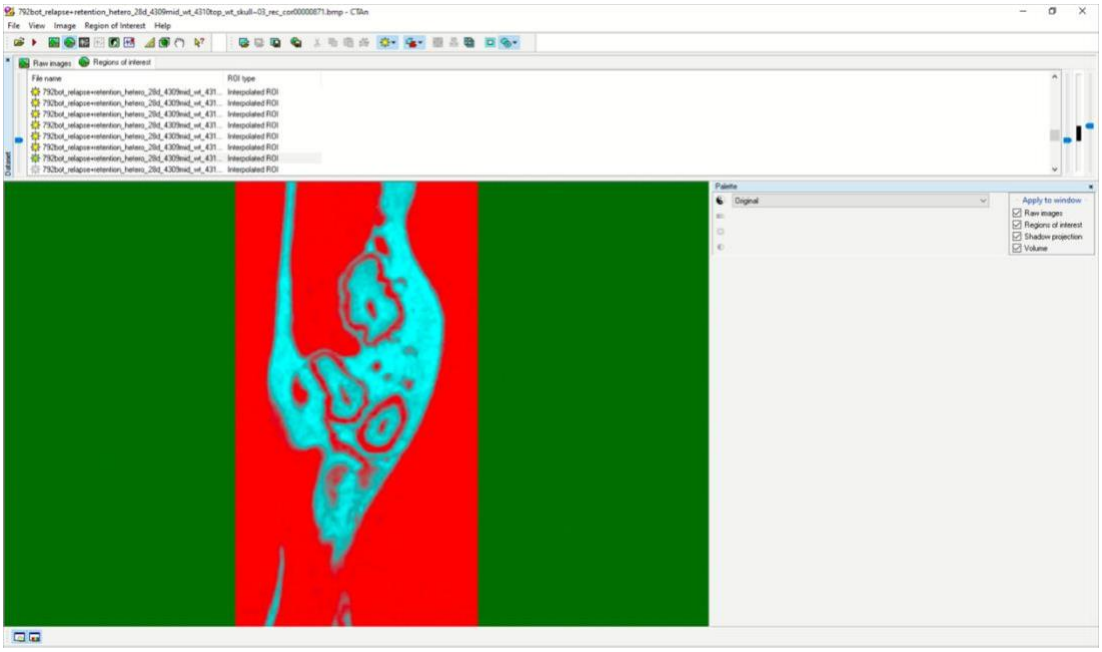

8. Scroll back to the first slice that represents the top of the region of interest.

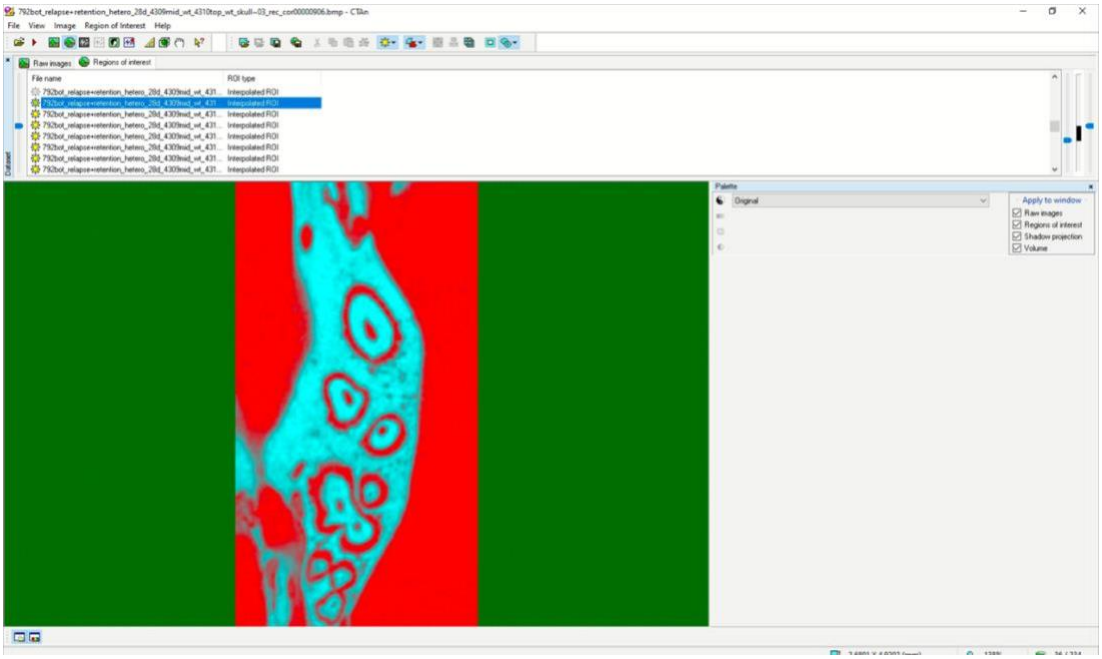

9. Select the square shape to define the area of interest.

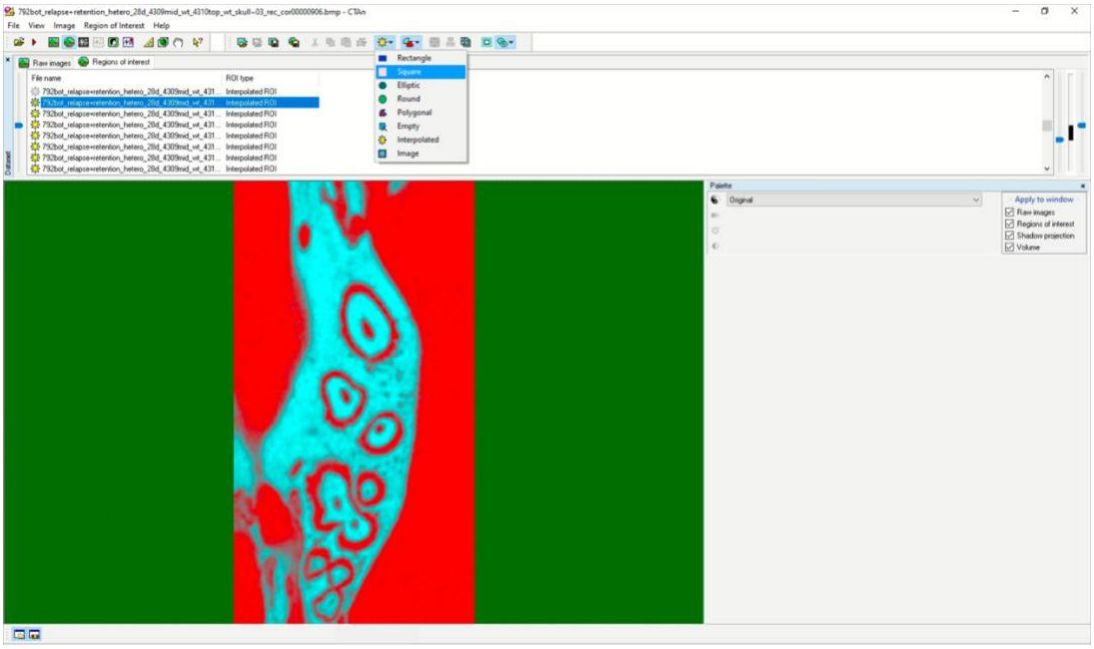

10. Select Dynamic interpolation

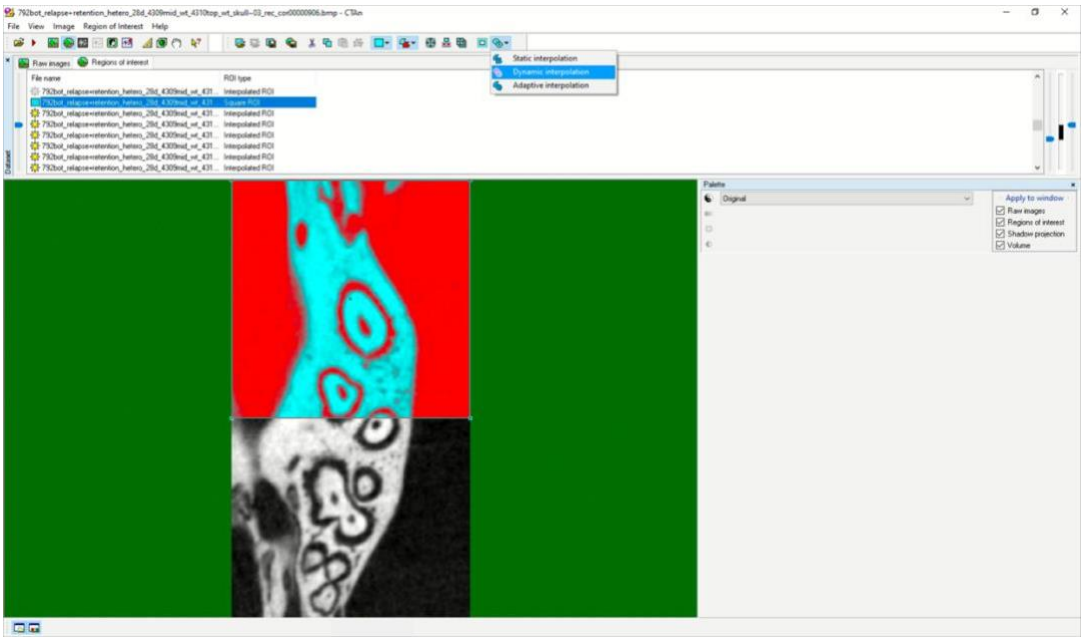

11. Shrink the square region of interest to be 0.35 by 0.35 mm. Position the square adjacent to the palatal root and be sure to note the square is not in the PDL space of the palatal root or distal root.

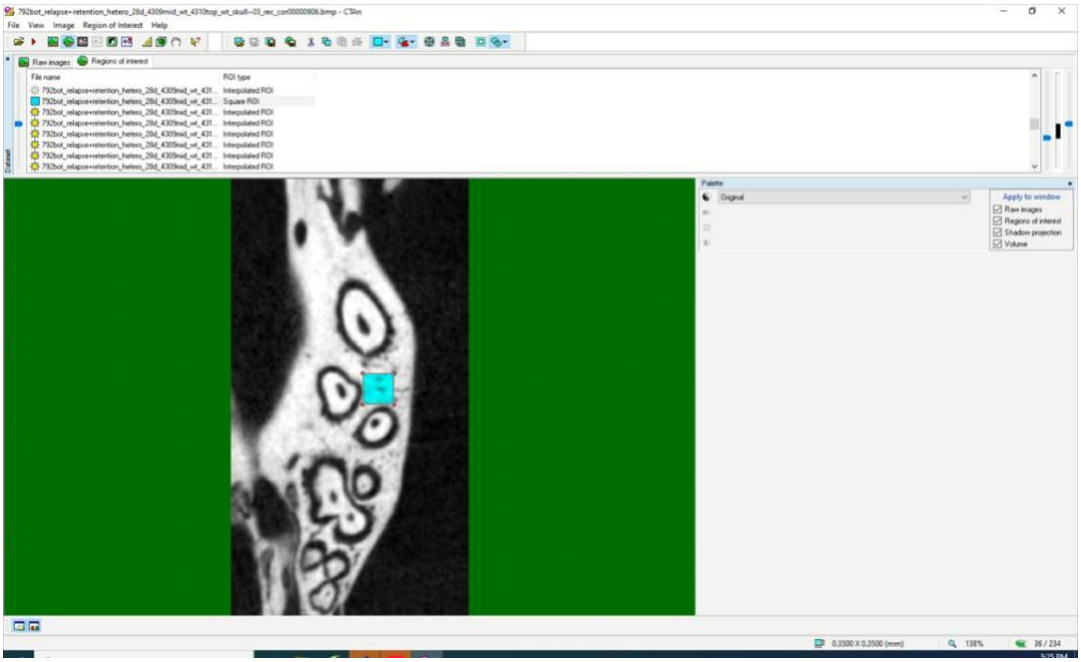

12. Scroll to the last slice and most the position to be adjacent to the palatal root.

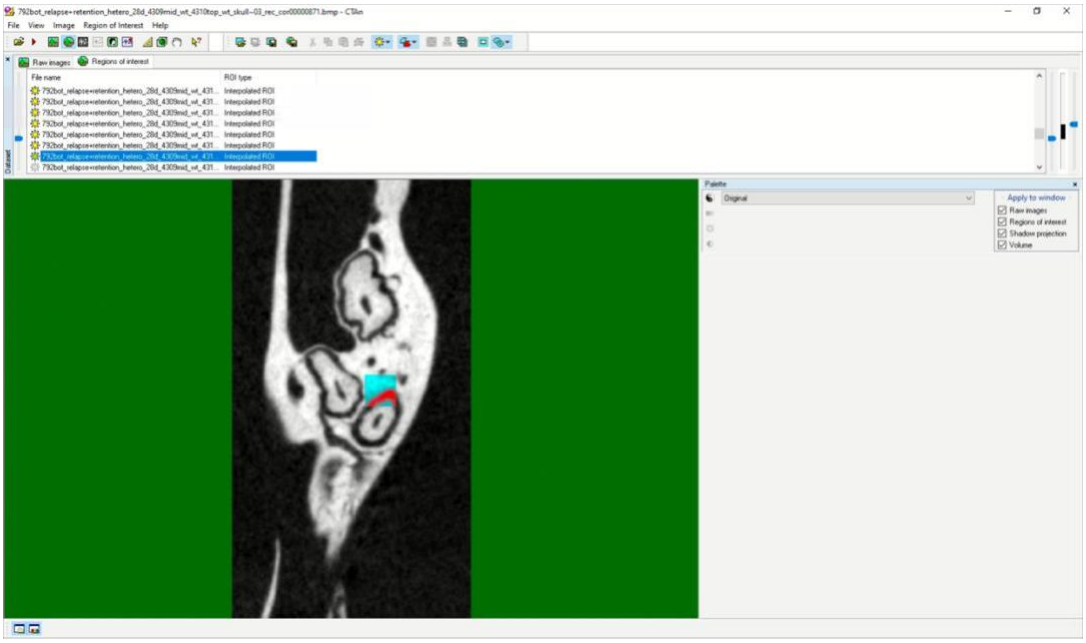

13. Select square again to have access to move the region of interest out of the PDL space.

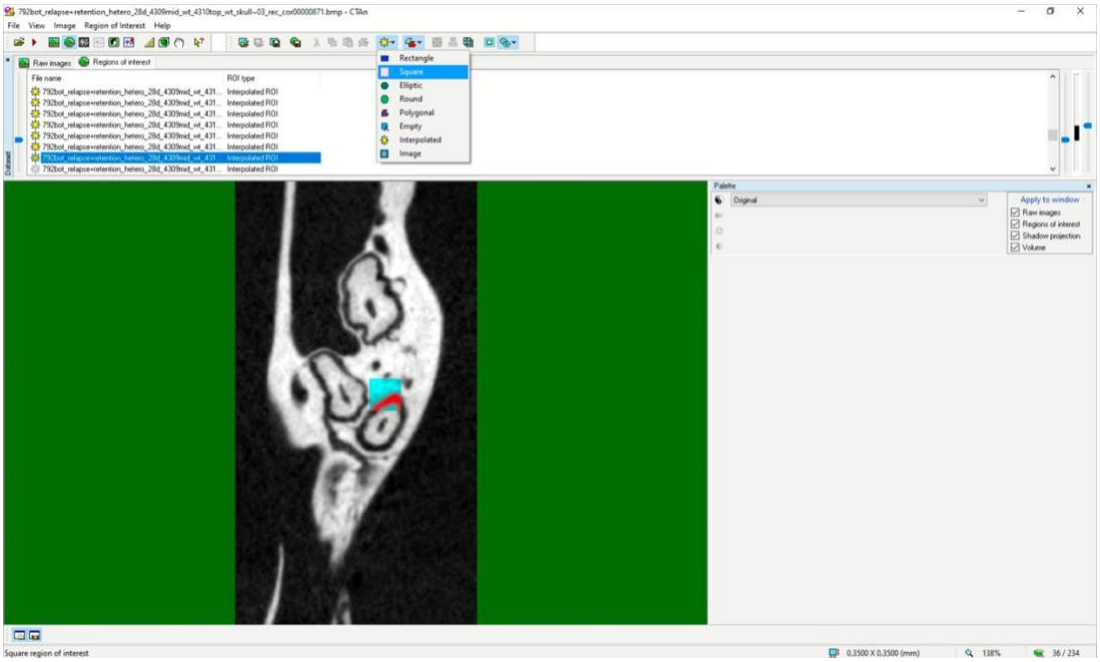

14. Move the region of interest to adjacent to the palatal root and make sure it is not in the PDL.

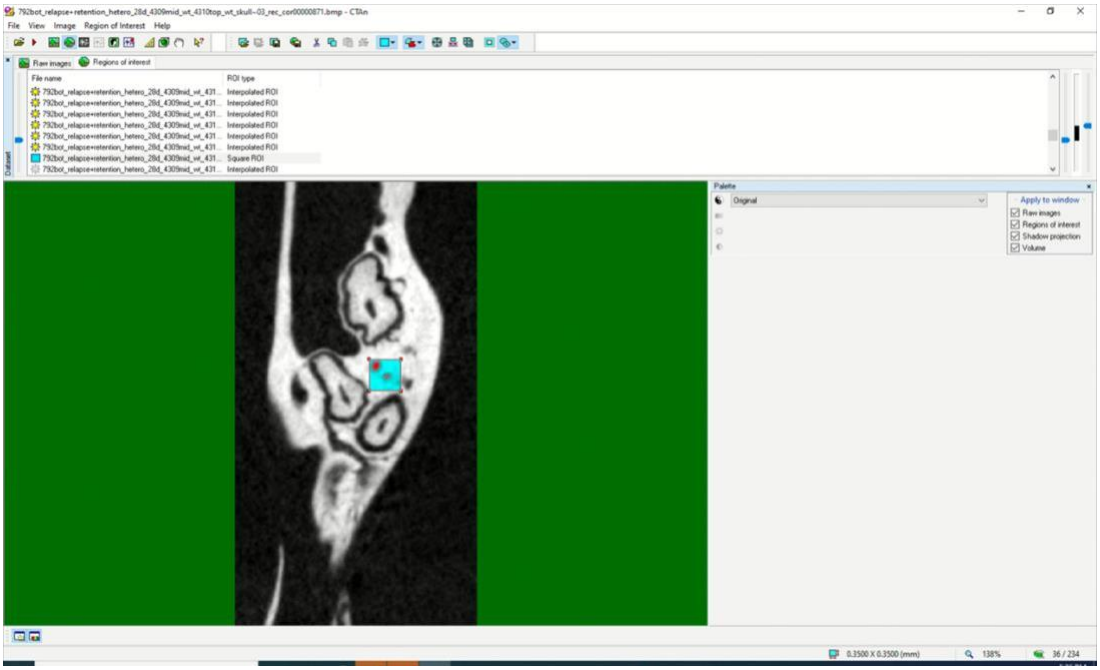

15. Scroll through all the samples to make sure the region of interest is not within the PDL of the root.

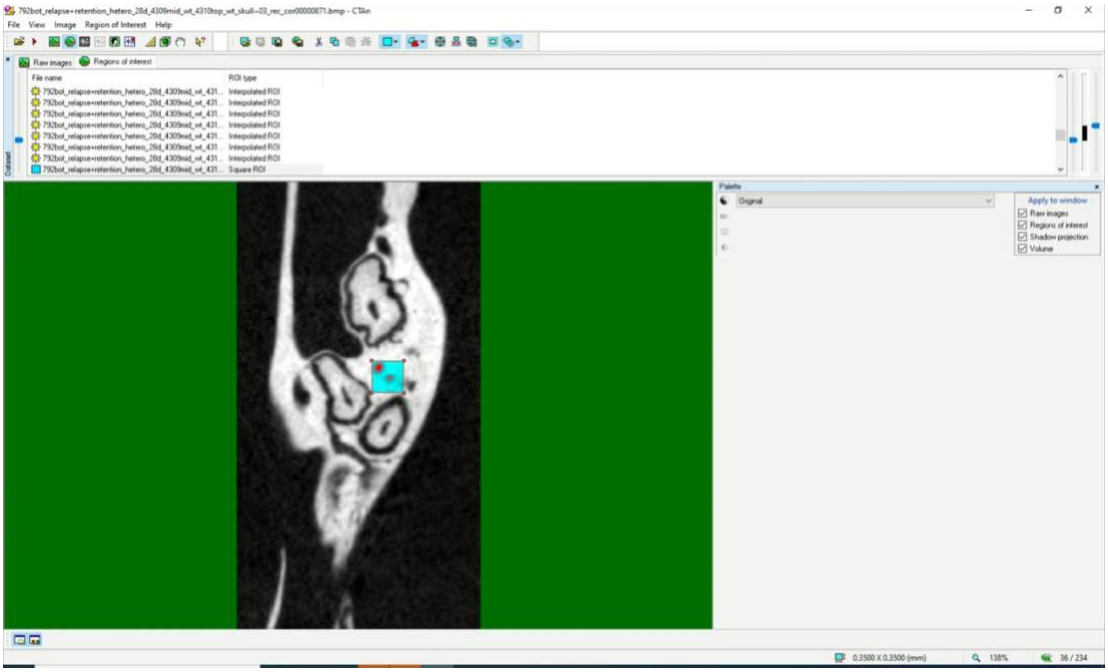

16. Then select the next tab **Binary Selection**. Set range for scale: **80 to 255**

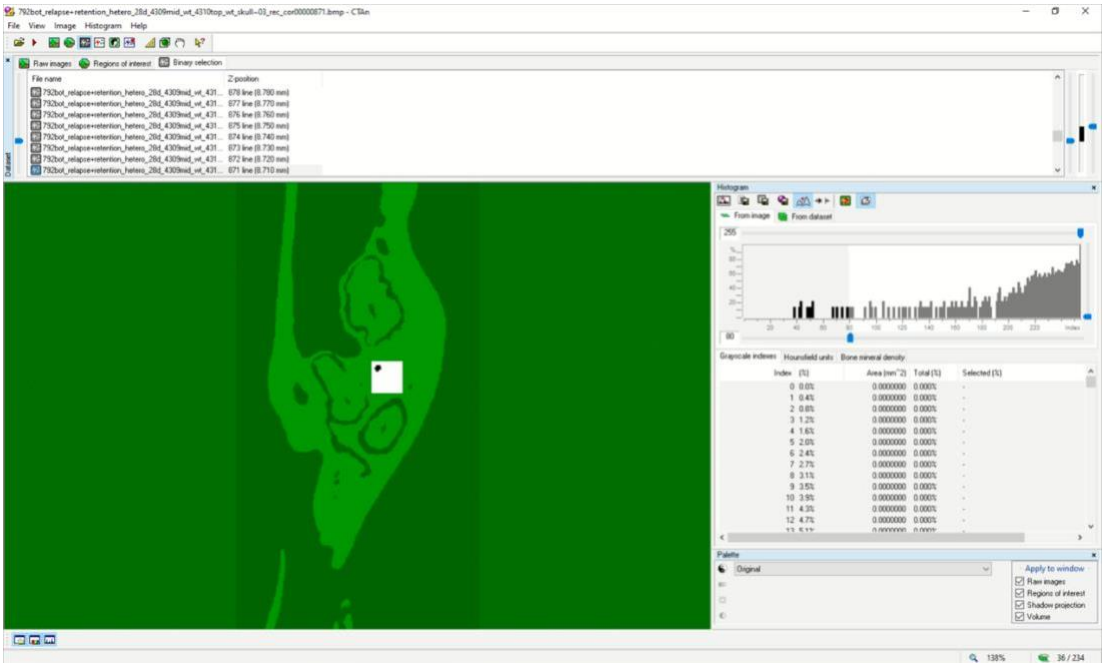

17. Select **Density range calibration.** Set the HU units to **-1000** to **9800.** Click **OK.**

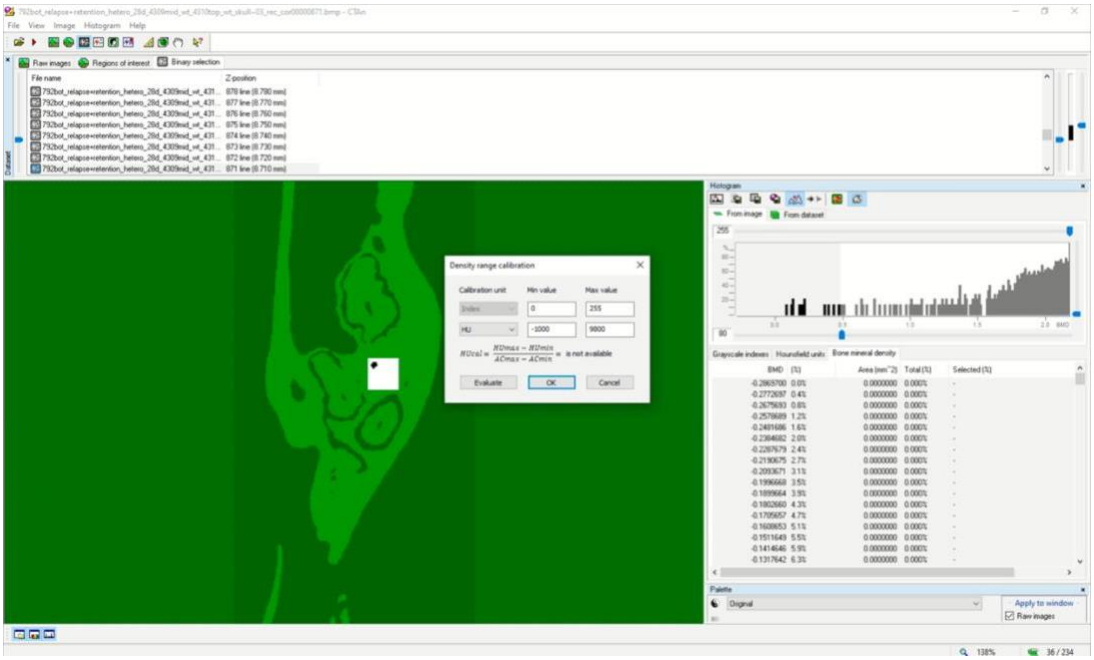

18. Click on File → Preferences → Histogram
a. Enter the values: **252.945 and 4366.11767.** Click **OK.**

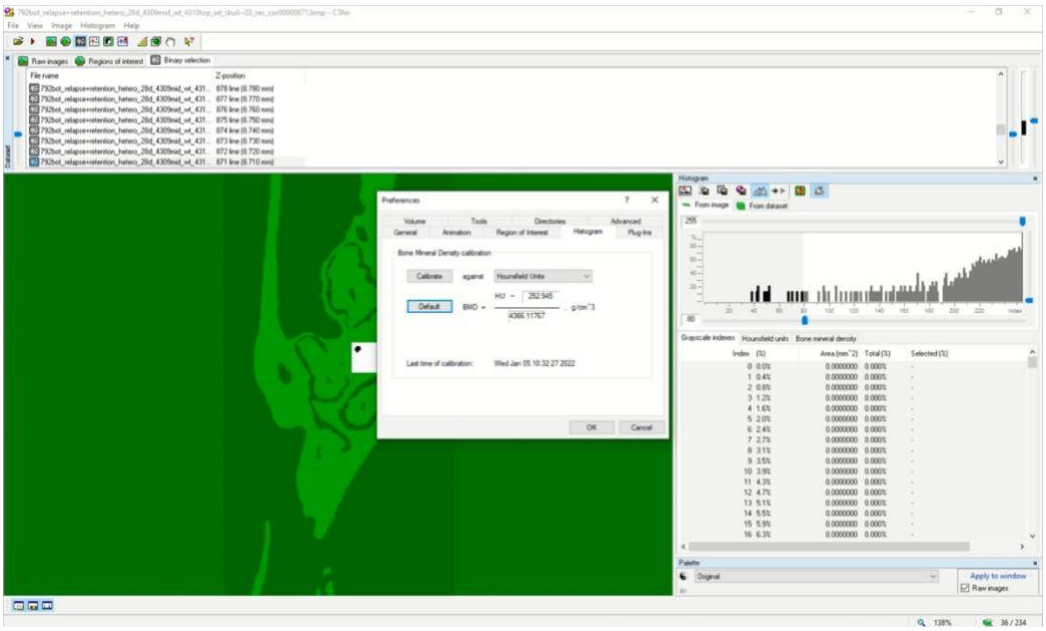

19. Select **From Dataset**

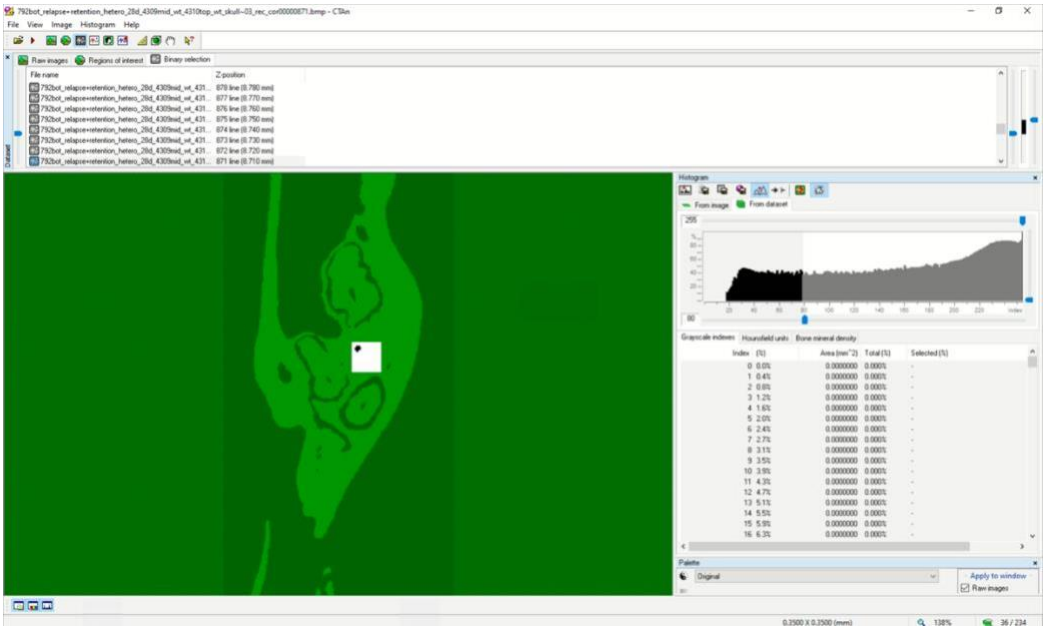

20. Select **Save histogram**

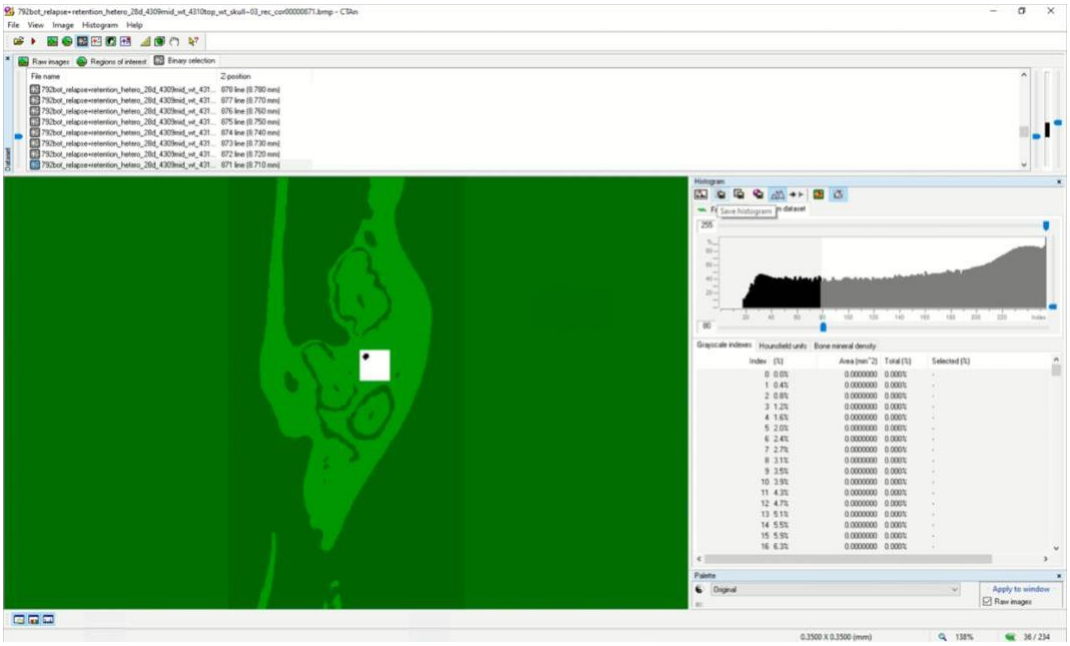

21. Select the folder to save the values from the volumetric data. Click **Save**

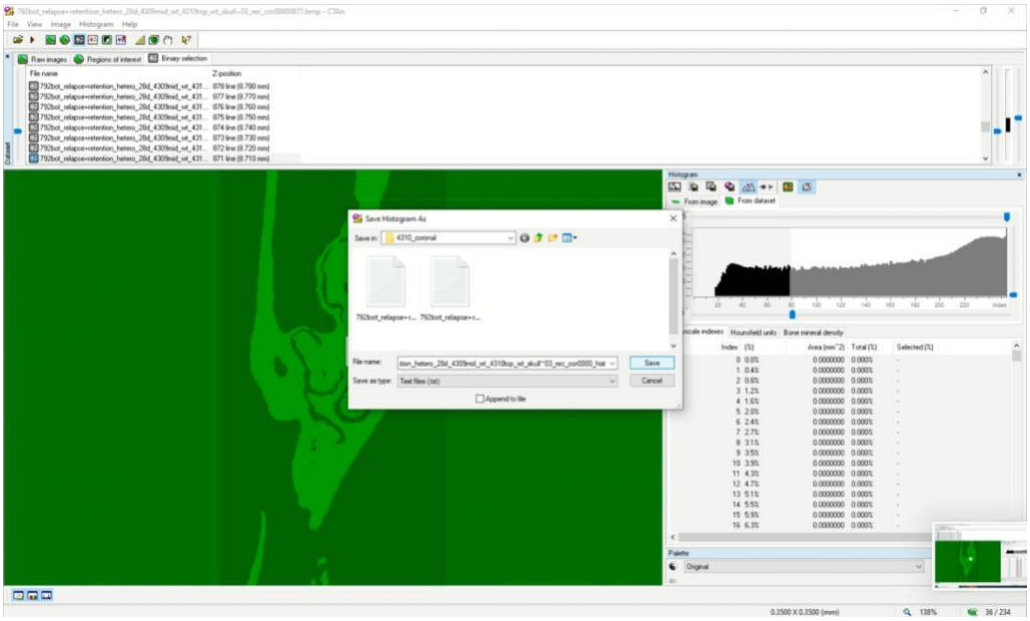

22. Select the next tab **Morphometry**

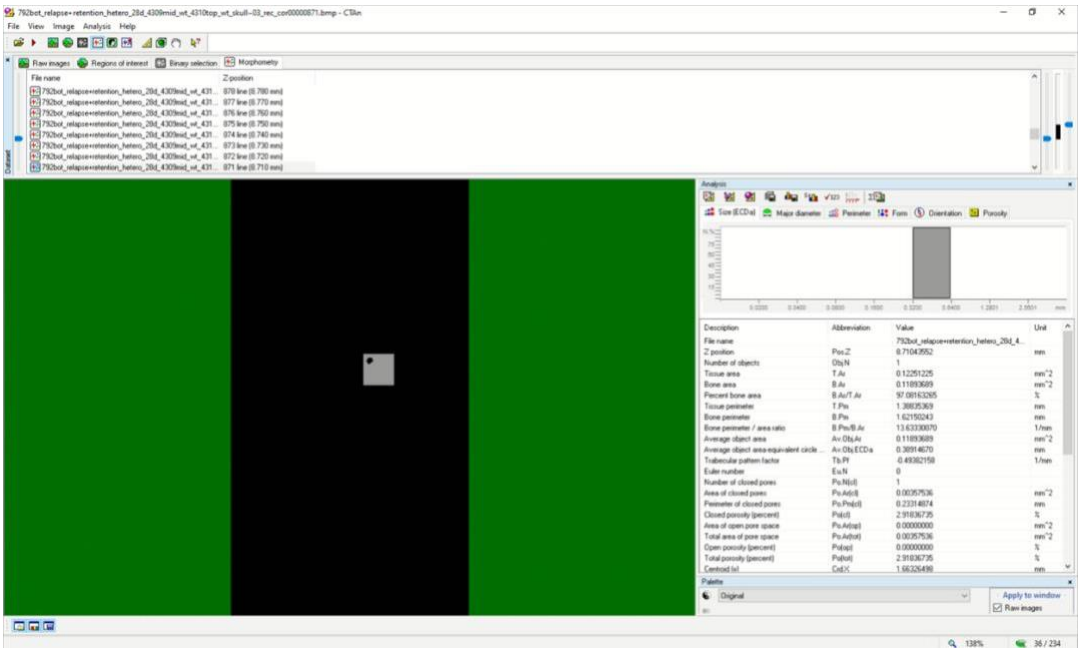

23. Select **3D analysis**

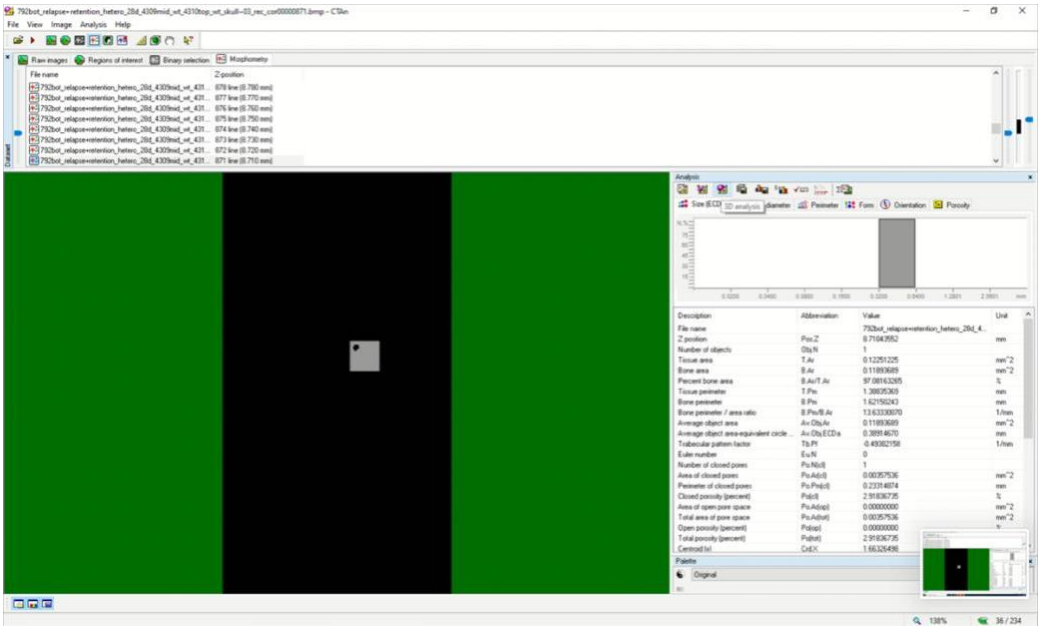

24. Keep the **Basic Values** checked. Click **Continue**

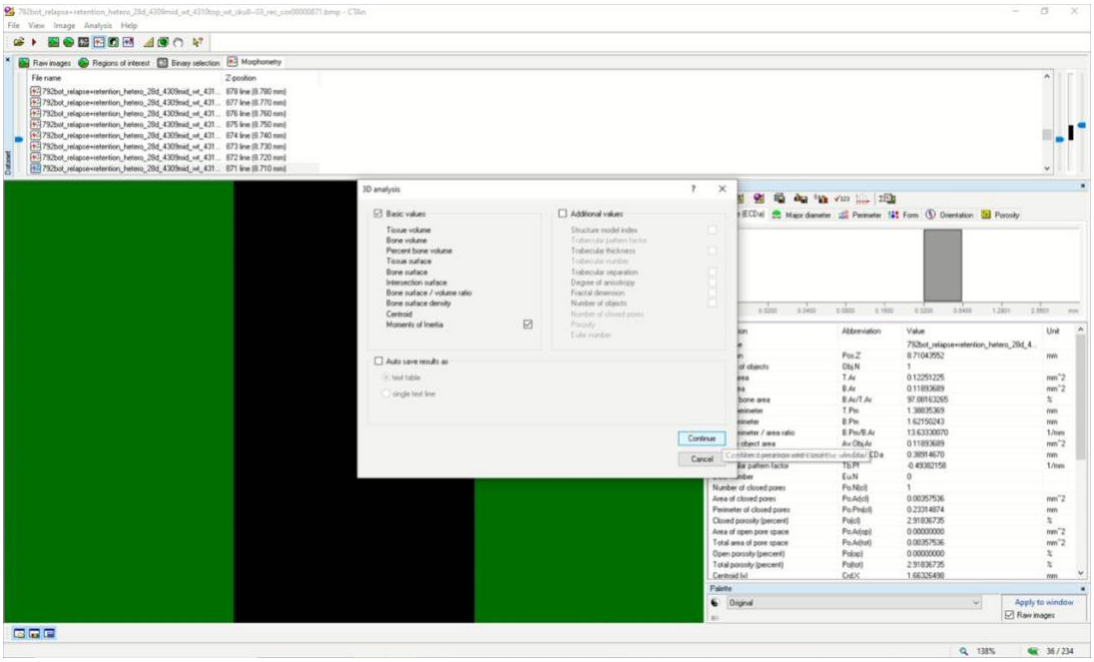

25. In the pop-up dialogue box 3D Analysis Results, select the **save histogram** icon.

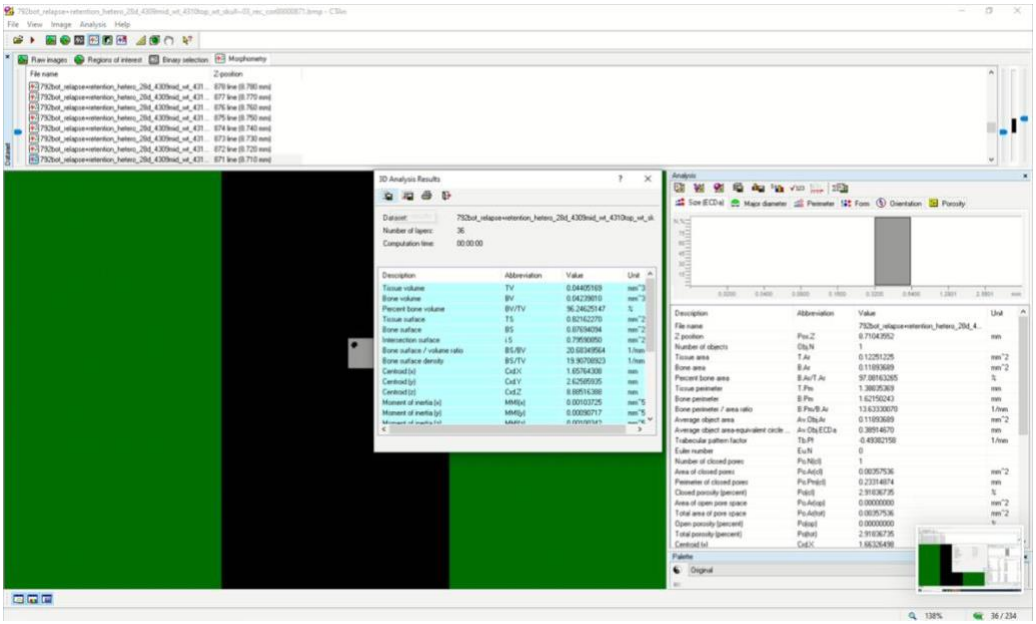

26. Select the folder desired and **Save** the results

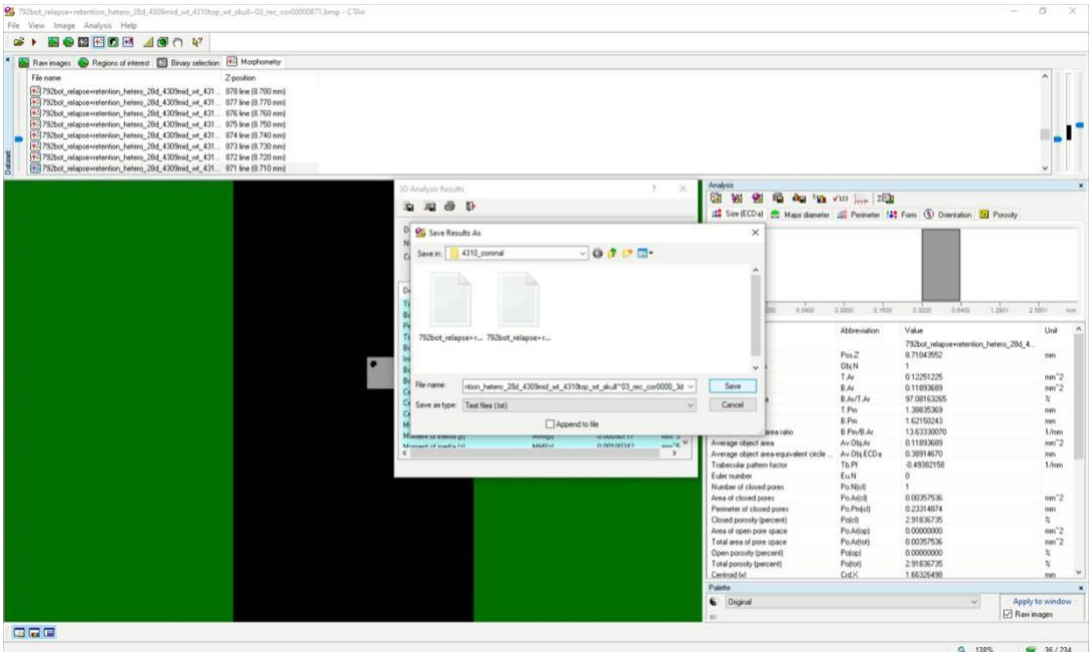

27. Find the value for **BMD** under the selection, listed as the mean. Enter this value into an excel spreadsheet to keep values organized per sample.

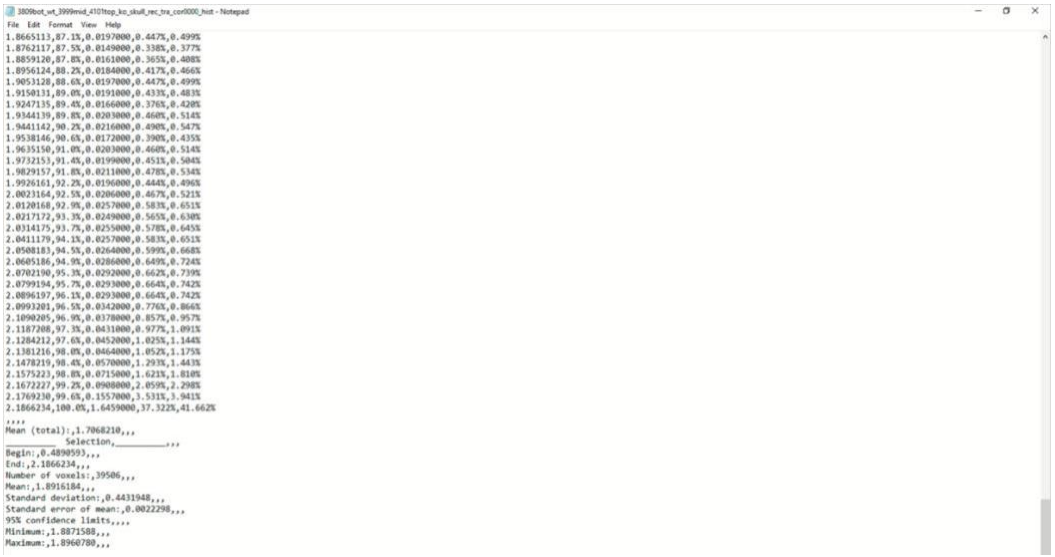

```
1.8665113,87.1%,0.0197000,0.447%,0.499%
1.8762117,87.5%,0.0149000,0.338%,0.377%
1.8859126,87.8%,0.0161000,0.365%,0.408%
1.8956124,88.2%,0.0184000,0.417%,0.466%
1.9053128,88.6%,0.0197000,0.447%,0.499%
1.9150131,89.0%,0.0191000,0.433%,0.483%
1.9247135,89.4%,0.0166000,0.376%,0.420%
1.9344139,89.8%,0.0203000,0.460%,0.514%
1.9441142,90.2%,0.0216000,0.490%,0.547%
1.9538146,90.6%,0.0172000,0.390%,0.435%
1.9635150,91.0%,0.0203000,0.460%,0.514%
1.9732153,91.4%,0.0199000,0.451%,0.504%
1.9829157,91.8%,0.0211000,0.478%,0.534%
1.9926161,92.2%,0.0196000,0.444%,0.496%
2.0023164,92.5%,0.0206000,0.467%,0.521%
2.0120168,92.9%,0.0257000,0.583%,0.651%
2.0217172,93.3%,0.0249000,0.565%,0.630%
2.0314175,93.7%,0.0255000,0.578%,0.645%
2.0411179,94.1%,0.0257000,0.583%,0.651%
2.0508183,94.5%,0.0264000,0.599%,0.668%
2.0605186,94.9%,0.0286000,0.649%,0.724%
2.0702190,95.3%,0.0292000,0.662%,0.739%
2.0799194,95.7%,0.0293000,0.664%,0.742%
2.0896197,96.1%,0.0293000,0.664%,0.742%
2.0993201,96.5%,0.0342000,0.776%,0.866%
2.1090205,96.9%,0.0378000,0.857%,0.957%
2.1187208,97.3%,0.0431000,0.977%,1.091%
2.1284212,97.6%,0.0452000,1.025%,1.144%
2.1381216,98.0%,0.0464000,1.052%,1.175%
2.1478219,98.4%,0.0570000,1.293%,1.443%
2.1575223,98.8%,0.0715000,1.621%,1.810%
2.1672227,99.2%,0.0908000,2.059%,2.298%
2.1769230,99.6%,0.1557000,3.531%,3.941%
2.1866234,100.0%,1.6459000,37.322%,41.662%
,,,,
Mean (total):,1.7068210,,,
Selection,_____,,,
Begin:,0.4890593,,,
End:,2.1866234,,,
Number of voxels:,39506,,,
Mean:,1.8916184,,,
Standard deviation:,0.4431948,,,
Standard error of mean:,0.0022298,,,
95% confidence limits,,,,
Minimum:,1.8871588,,,
Maximum:,1.8960780,,,
```

28. Find the value for **BV and BV/TV** under the selection, listed as the mean. Enter this value into an excel spreadsheet to keep values organized per sample.

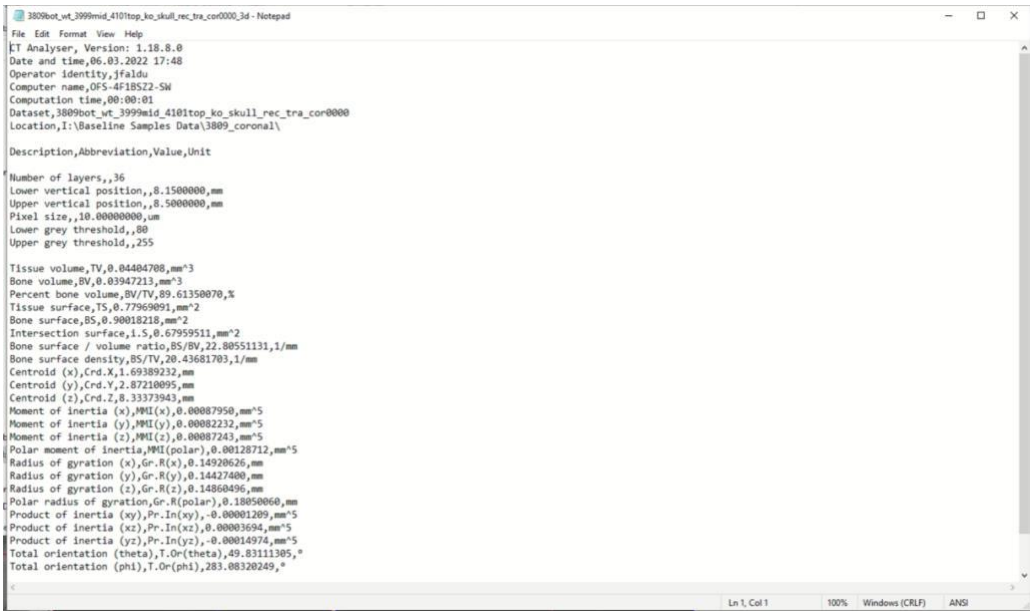

For measuring root volume, the CTAn software was used again to measure the volumetric quantification of the mesial root of the maxillary left first molar.

1. Follow the CTAn protocol above to open the file
2. Starting from the apical, scroll and find the file that shows the first speck of the mesial root apex (set bottom of selection); (when the mesial root joins the palatal root→set top of selection)
3. Select the Interpolated Shape & Dynamic interpolation to define the area of interest
4. Trace every slice, outlining the mesial root, from the bottom of selection to the top of selection to encircle the root volume

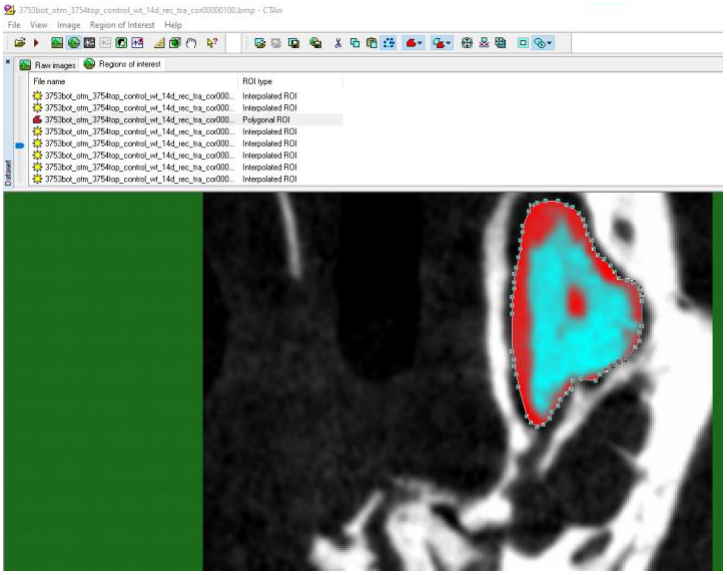

5. Scroll through all the sample slices to make sure the ROI is within the PDL and includes the entire root and omits bone. Click “Edit Polygonal”. You may have to adjust your tracing points or trace an additional slice
6. In the histogram, records the Tissue Volume result as the root volume

4.8 Statistical Analysis

Statistical evaluation was performed with the program GraphPad Prism (V9.3.1). Data was expressed as means and standard deviations for each group and subjected to two-way ANOVA followed by a Tukey test for multiple comparisons among the Dmp1-Cre$^{-/-}$;Tbr2$^{fl/fl}$ and Dmp1-Cre$^{+/-}$;Tbr2$^{fl/fl}$ groups (p=0.05). For Aim 3, data is expressed in the same way as above but was analyzed using a one-way ANOVA. P values of <0.05 were considered statistically significant.

5. RESULTS

5.1 OTM

For Aim 1, in the OTM group, KO mice had statistically significantly more OTM (57%) than WT mice (**p=0.001). KO OTM mice on average measured 232μm and WT OTM mice on average measured 148μm. Control mice in the KO and WT group showed no OTM. The control represents mice that did not receive the orthodontic spring appliance, therefore the distances between the first and second maxillary left molar is zero. Figure 5 depicts this data, with the light blue bar indicating WT mice and the dark blue bar indicating KO mice. 3 samples were excluded due to distal molar breakage during spring removal or residual composite in between M1 and M2

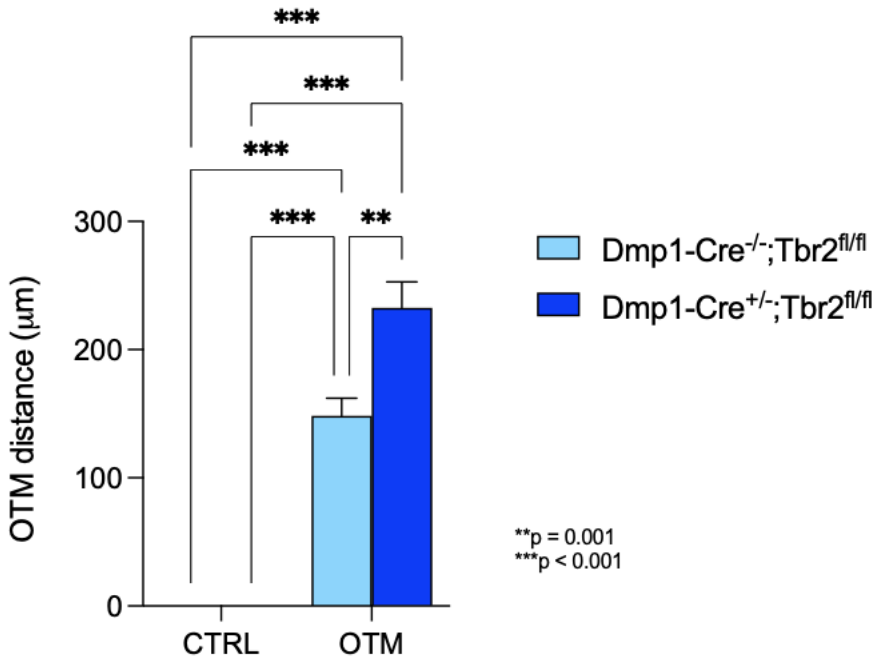

Figure 5: OTM distance (μm) measurements for KO and WT experimental and control groups.

5.2 Alveolar Bone Remodeling

For Aim 2, BV/TV measurements (%) showed that KO mice had less BV/TV than WT mice in both the CTRL and OTM groups, although not statistically significant. WT CTRL, KO CTRL, WT OTM, and KO OTM measured 71.2%, 64.8%, 64.3%, and 60.1% respectively.

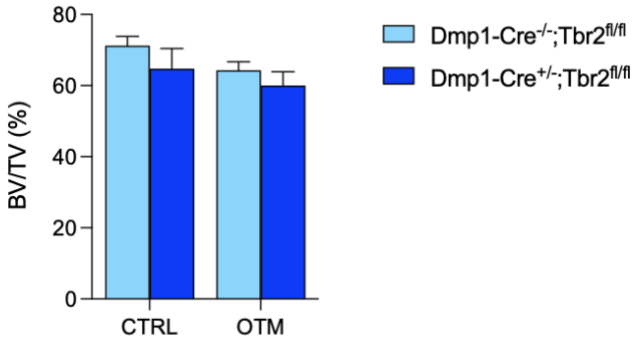

Figure 6: BV/TV (%) measurements for KO and WT experimental and control groups.

For Aim 2, BMD measurements (g/cm^3) showed that KO mice had statistically significantly less BMD compared to WT mice in both control and OTM groups (*p<0.05). WT CTRL, KO CTRL, WT OTM, and KO OTM measured 1.60g/cm^3, 1.30g/cm^3, 1.44g/cm^3, and 1.15g/cm^3 respectively.

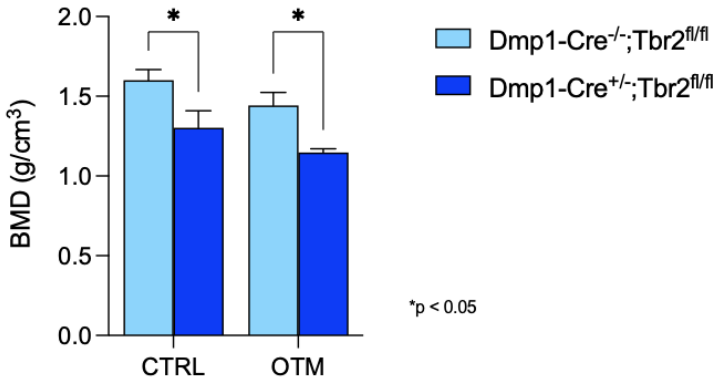

Figure 7: BMD (g/cm^3) measurements for KO and WT experimental and control groups.

For Aim 2, ABH loss measurements (mm) showed that KO mice had similar ABH levels as the WT mice in the control group. In the OTM group, KO mice had more ABH loss than WT mice, although not statistically significant. WT CTRL, KO CTRL, WT OTM, and KO OTM measured 0.200mm, 0.208mm, 0.241mm, and 0.284mm respectively.

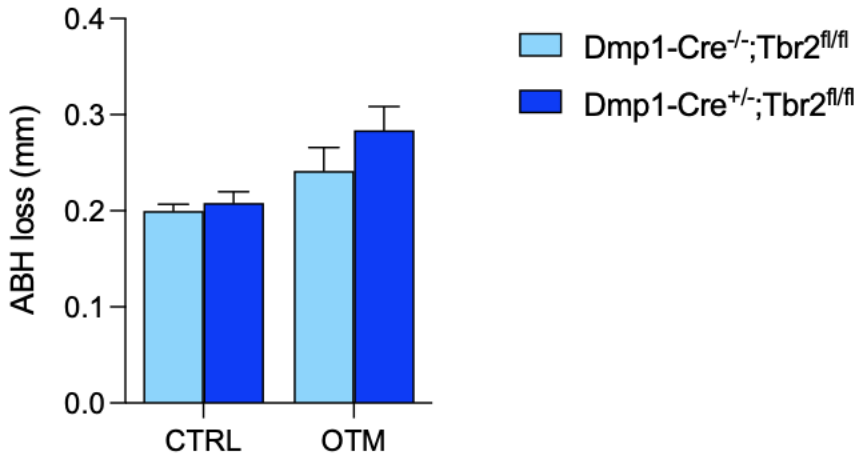

Figure 8: ABH loss (mm) measurements for KO and WT experimental and control groups.

5.3 Root Length and Root Volume

For Aim 2, root length measurements (mm) showed that KO mice had similar RL as WT mice in the control group. In the OTM group, KO mice had slightly shorter RL than WT mice, although not statistically significant. WT CTRL, KO CTRL, WT OTM, and KO OTM measured 1.18mm, 1.14mm, 1.14mm, and 1.02mm respectively.

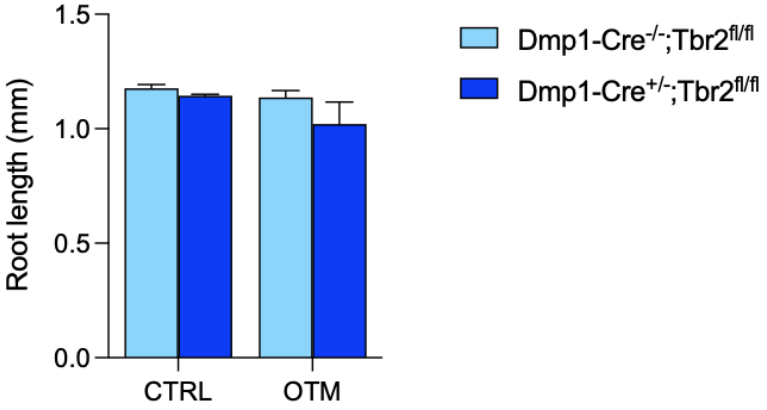

Figure 9: Root length (mm) measurements for KO and WT experimental and control groups.

For Aim 2, root volume measurements (mm^3) showed that KO mice had similar RV as WT mice in the control group. In the OTM group, KO mice had slightly smaller RV than WT mice, although not statistically significant. WT CTRL, KO CTRL, WT OTM, and KO OTM measured $0.223mm^3$, $0.223mm^3$, $0.226mm^3$, and $0.212mm^3$ respectively.

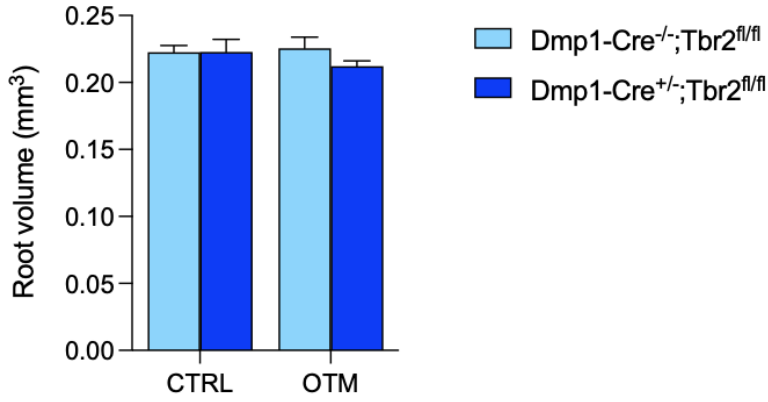

Figure 10: Root volume (mm^3) measurements for KO and WT experimental and control groups.

5.4 Aim 3 Retention-Relapse Model

For Aim 3, we were able to replicate baseline retention relapse measurements in a mouse model. The 14 day OTM, 14 day OTM with 14 day retention, 14 day OTM with 14 day retention and 7 day relapse, and 28 day OTM groups measured 196μm, 293μm, 118μm, and 537μm respectively. Our results show that the 28 day OTM group had statistically significantly more OTM compared to all the other groups (*$p<0.05$). There is a decrease in OTM for the relapse group by 60% from the retention group and by 40% from the 14 day OTM group. We are seeing more OTM in the retention group compared to the 14d OTM group, indicating that the retainer is not fully deactivating the spring forces. However, it is significantly reducing the mesialization force when compared to the 28 day OTM group.

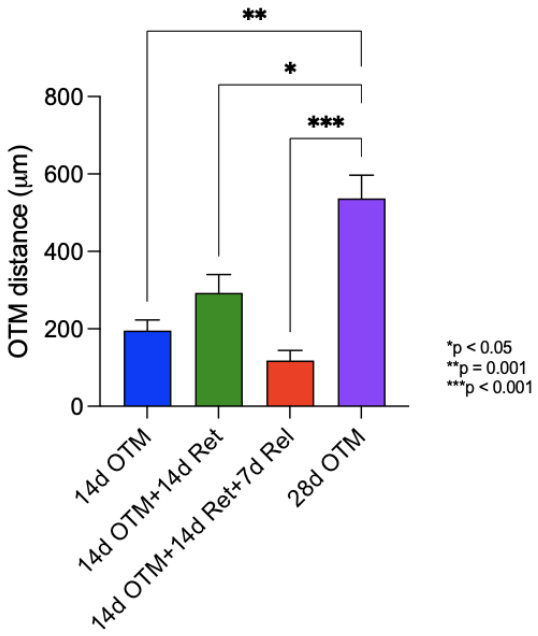

Figure 11: OTM distances for the orthodontic tooth movement, retention, and relapse model groups.

6. DISCUSSION

In our experimental OTM group for our WT mice, our average OTM values (148um) were comparable to those found in the OTM literature [24]. Thus, we can conclude that our surgical set up, orthodontic spring appliance application, and procedural timeline are accurate and reproducible.

Initially, we had hypothesized that the KO mice have less OTM due to the disruption in the osteocyte signaling pathway, with downstream effects that ultimately decrease RANKL production needed for osteoclastogenesis [4]. With fewer osteoclasts, we anticipated slower bone turnover, and thus, less OTM. However, our results showed that the KO mice had 57% more OTM than the WT mice counterparts. Thus, this highlights the fact that TGF-β is a complex signaling molecule with pleiotropic effects on multiple cell types. The signaling pathway of TGF-β is very intricate, as previous studies have shown TGF-β to be secreted by osteoblasts, osteoclasts, and osteocyte cells. Moreover, there exists TGF-β receptors not only on osteocytes, but on osteoblasts and osteoclast cells [23]. The studies by Tang et. al. and Dole et. al., have confirmed that TGF-β is known to exert diverse effects on all bone cell types: osteoclasts, osteoblasts, and their progenitor cells to coordinate bone remodeling. The TGF-β molecule itself can serve as a chemotactic agent in the extracellular matrix, dictating the differentiation of different osteoprogenitor cells [23]. Thus, since our study only focused on targeting the TGF-β receptor on osteocyte cells, there may be other active TGF-β on osteoblasts and osteoclasts, or even active TGF-β molecules present in the extracellular matrix. TGF-β is involved with the intricate coupling of osteoblast and osteoclast activity, which holds a fine balance with the transcribed molecular factors such as RANKL, OPG, MMP, and CatK [23]. It is possible that

since TGF-β is so complex and broad-acting in its function, any disruption in its signaling pathway can cause dysregulation in bone homeostasis and perilacunar remodeling.

Since osteocyte cells are the key regulators of bone turnover through PLR and its mechano-sensing abilities, if there are any disruptions to its normal functioning capabilities, we may see a disruption of the balance of bone turnover and the normal signaling cascades. This dysregulation of bone remodeling may be the reason why we are seeing more OTM in the KO group. With osteocyte cells being uncontrolled, bone may be quickly degraded and immature, porous bone may be laid down in its place, causing to tooth to move quicker through this softer bone. We also saw a large variation in OTM values in the male Dmp1-Cre$^{+/-}$;Tbr2$^{fl/fl}$ group, with the lowest value being 144μm and the largest value being 310μm. This supports the fact that a defect in TGF-β signaling makes bone remodeling unpredictable and variable, since the process has been dysregulated.

Another theory as to why we may be seeing increased OTM in the KO mice group is because the role of TGF-β itself not only affects the hard tissue bone, but also soft tissue such as the periodontal ligament. Stemmler et. al. confirmed that TGF-β broadly affects the periodontium in terms of the soft tissue, through the PDL cells themselves. With changes in the PDL fibers, the pressure-tension theory of orthodontic tooth movement may be altered, causing the KO mice molars to move greater through the alveolar bone.

For Aim 2 regarding alveolar bone remodeling, our results match with the results we saw with our Aim 1 OTM findings. KO mice had less BV/TV percentages compared to the WT mice in both the CTRL and OTM groups. In addition, KO mice had less BMD values compared to the WT mice in both the CTRL and OTM groups, which was statistically significant. With the KO

mice having less BV/TV and BMD, we can expect the OTM rate to be faster in the KO mice group, which is congruent with our OTM results in Aim 1.

In regards to alveolar bone height loss, our results showed that KO mice had similar ABH levels as WT mice in the control group. Since there is no OTM being applied to this group, we expect the bone levels to be similar. In the OTM group, we found the KO mice had more ABH loss than the WT mice. This is expected to occur with orthodontic tooth movement, as the bone is remodeling and moving at a quicker rate in the KO group, in addition to the TGF-β signaling being dysregulated, the increased ABH loss in this group matches these findings.

In regards to root length and root volume, the control groups showed that the KO mice group had similar RL and RV values compared to the WT mice group. Since there is no OTM being applied to this group, we expect the root measurement parameters to be similar. In the OTM group, the KO mice group had shorter RL and smaller RV compared to the WT mice group. These findings are anticipated, as with increased OTM in the KO group, we will observe a higher risk of root resorption, causing a decrease in RL and RV. Root shortening has been known to correspond with orthodontic tooth movement rate, and since our results are not statistically significant, we can conclude that the decrease in RL and RV is not necessarily due to a dysfunction in TGF-β signaling.

Lastly, for Aim 3, we were able to reproduce a retention-relapse model in mice. The measurement trends were what we had predicted to see: the relapse group had less OTM than the 14 day OTM group (40% decrease), and the 28 day OTM group had more than double the OTM than the 14 day OTM group. We had hoped that the retention group would be able to hold the same amount of OTM as the 14 day group, however, our results showed that the retention group had slightly more OTM than the 14 day OTM group. These findings show that the retainer is

functioning in preventing further OTM, but not completely. When compared to the 28 day OTM group, the retention group is significantly reducing the anticipated OTM. However, the retention group is still allowing some additional OTM to occur, so our composite retainer device may not be completely retaining the final OTM. This may be due to the composite not being fully applied into all of the coils of the spring. Surgically, it was difficult to isolate the area in the oral cavity, and place the flowable composite throughout the entire spring assembly from the incisors up to the first molar. Thus, we will need to refine our retention appliance to ensure that true retention can be implemented in future studies.

6.1 Clinical Implications

With our current data, we hope to analyze the samples under histological cross sections to determine how the cells are responding on a molecular level, which could help elucidate the function of TGF-β directly. With these signaling pathways decoded and osteocyte cell function controlled, we can clinically develop targeted molecular therapy that can increase tooth movement safely with respect to the periodontium, while maintaining retention and minimizing the amount of relapse.

6.2 Limitations

Throughout the course of the study, we encountered various limitations. Due to the difficulty in breeding the transgenic KO mice and high demand for this mouse line, acquiring KO mice for KO control group was limited. From the surgical standpoint in placing the orthodontic spring appliance, isolation was challenging. Multiple samples suffered cheek laceration and post-operative pain, ultimately resulting in mice mortality. Spring placement was also unpredictable, as some samples would have appliances dislodged mid-way through the time

point. Samples with residual composite between the molars that bonded to the second molars were excluded, as well as cracked first molars upon spring removal.

6.3 Future Directions

For future studies, increasing the sample size can help to normalize the data, decrease variation, and increase the power of the study. We can also suggest looking at the contralateral upper right molars as a control and seeing if there are any bony changes in remote sites of the maxilla. Another interesting approach would be to target different stages of orthodontic tooth movement, such as retention or relapse, and seeing if there are genetic markers that can be manipulated to maximize retention or minimize relapse of tooth movements.

It would be interesting to confirm in the tissue where and how TGF-β expression is affected in this model and whether other TGF-β receptors (on osteoblasts or osteoclasts) are compensating for the disrupted osteocyte cell. We can also try to measure the quantity of other molecular factors like RANKL to see whether osteocyte loss of TGF-β signaling effects RANKL expression. To pinpoint the role of TGF-β in bone, replicating this study in osteoblast or osteoclast specific TGF-β knockouts would give us a better understanding of TGF-β function.

The present study used ex-vivo microCT imaging to evaluate OTM and alveolar bone quality. In-vivo microCT imaging would be more accurate at measuring initial bone and tooth data within the same sample. With in-vivo imaging, scans can be conducted at different timepoints of the study; for example, a scan can be done on Day 3 and 7 to examine changes over time.

In order to provide true retention at the end of the OTM phase and to avoid the retainer from still providing some active OTM, it may be prudent to change the retainer device. Future

studies may consider removing the entire spring appliance completely and bonding a full composite bar as a retainer so serve as true retention.

7. CONCLUSIONS

- Our study confirmed that the osteocytes are a key player in bone turnover, and any disruption to its function can cause significant dysregulation of bone remodeling.
- *KO mice had 57% more OTM than WT mice.
- KO mice had slightly less BV fraction compared to WT mice in the control and OTM groups.
- *KO mice had significantly less BMD compared to WT mice in the control and OTM groups.
- KO mice had more ABH loss compared to WT mice in the OTM group.
- KO mice had less RL and RV compared to WT mice in the OTM group.
- A relapse-retention model can be successfully reproduced in a mouse model, but refinements should be made to improve the efficacy of the retention appliance.

8. REFERENCES

1. Bonewald LF. The amazing osteocyte. J Bone Miner Res. 2011 Feb;26(2):229-38. doi: 10.1002/jbmr.320. PMID: 21254230; PMCID: PMC3179345.

2. Burger EH, Klein-Nulend J, Smit TH. Strain-derived canalicular fluid flow regulates osteoclast activity in a remodelling osteon--a proposal. J Biomech. 2003 Oct;36(10):1453-9. doi: 10.1016/s0021-9290(03)00126-x. PMID: 14499294.

3. Cheung T, Park J, Lee D, Kim C, Olson J, Javadi S, Lawson G, McCabe J, Moon W, Ting K, Hong C. Ability of mini-implant-facilitated micro-osteoperforations to accelerate tooth movement in rats. Am J Orthod Dentofacial Orthop. 2016 Dec;150(6):958-967. doi: 10.1016/j.ajodo.2016.04.030. PMID: 27894545; PMCID: PMC5131371.

4. Dole NS, Mazur CM, Acevedo C, Lopez JP, Monteiro DA, Fowler TW, Gludovatz B, Walsh F, Regan JN, Messina S, Evans DS, Lang TF, Zhang B, Ritchie RO, Mohammad KS, Alliston T. Osteocyte-Intrinsic TGF-β Signaling Regulates Bone Quality through Perilacunar/Canalicular Remodeling. Cell Rep. 2017 Nov 28;21(9):2585-2596. doi: 10.1016/j.celrep.2017.10.115. PMID: 29186693; PMCID: PMC6014615.

5. Franz-Odendaal TA, Hall BK, Witten PE. Buried alive: how osteoblasts become osteocytes. Dev Dyn. 2006 Jan;235(1):176-90. doi: 10.1002/dvdy.20603. PMID: 16258960.

6. Henneman S, Von den Hoff JW, Maltha JC. Mechanobiology of tooth movement. Eur J Orthod. 2008 Jun;30(3):299-306. doi: 10.1093/ejo/cjn020. PMID: 18540017.

7. Jacobs CR, Temiyasathit S, Castillo AB. Osteocyte mechanobiology and pericellular mechanics. Annu Rev Biomed Eng. 2010 Aug 15;12:369-400. doi: 10.1146/annurev-bioeng-070909-105302. PMID: 20617941.

8. Kamioka H, Honjo T, Takano-Yamamoto T. A three-dimensional distribution of osteocyte processes revealed by the combination of confocal laser scanning microscopy and differential interference contrast microscopy. Bone. 2001 Feb;28(2):145-9. doi: 10.1016/s8756-3282(00)00421-x. PMID: 11182371.

9. Kamioka H, Ishihara Y, Ris H, Murshid SA, Sugawara Y, Takano-Yamamoto T, Lim SS. Primary cultures of chick osteocytes retain functional gap junctions between osteocytes and between osteocytes and osteoblasts. Microsc Microanal. 2007 Apr;13(2):108-17. doi: 10.1017/S143192760707016X. PMID: 17367550.

10. Matsumoto T, Iimura T, Ogura K, Moriyama K, Yamaguchi A. The role of osteocytes in bone resorption during orthodontic tooth movement. J Dent Res. 2013 Apr;92(4):340-5. doi: 10.1177/0022034513476037. Epub 2013 Jan 28. PMID: 23358677.

11. Munger JS, Huang X, Kawakatsu H, Griffiths MJ, Dalton SL, Wu J, Pittet JF, Kaminski N, Garat C, Matthay MA, Rifkin DB, Sheppard D. The integrin alpha v beta 6 binds and activates latent TGF beta 1: a mechanism for regulating pulmonary inflammation and fibrosis. Cell. 1999 Feb 5;96(3):319-28. doi: 10.1016/s0092-8674(00)80545-0. PMID: 10025398.

12. Murshid SA. The role of osteocytes during experimental orthodontic tooth movement: A review. Arch Oral Biol. 2017 Jan;73:25-33. doi: 10.1016/j.archoralbio.2016.09.001. Epub 2016 Sep 8. PMID: 27653146.

13. Nakashima T, Hayashi M, Fukunaga T, Kurata K, Oh-Hora M, Feng JQ, Bonewald LF, Kodama T, Wutz A, Wagner EF, Penninger JM, Takayanagi H. Evidence for osteocyte regulation of bone homeostasis through RANKL expression. Nat Med. 2011 Sep 11;17(10):1231-4. doi: 10.1038/nm.2452. PMID: 21909105.

14. Proff P, Römer P. The molecular mechanism behind bone remodelling: a review. Clin Oral Investig. 2009 Dec;13(4):355-62. doi: 10.1007/s00784-009-0268-2. Epub 2009 Mar 25. PMID: 19319579.

15. Robling AG, Niziolek PJ, Baldridge LA, Condon KW, Allen MR, Alam I, Mantila SM, Gluhak-Heinrich J, Bellido TM, Harris SE, Turner CH. Mechanical stimulation of bone in vivo reduces osteocyte expression of Sost/sclerostin. J Biol Chem. 2008 Feb 29;283(9):5866-75. doi: 10.1074/jbc.M705092200. Epub 2007 Dec 17. PMID: 18089564.

16. Rys JP, Monteiro DA, Alliston T. Mechanobiology of TGFβ signaling in the skeleton. Matrix Biol. 2016 May-Jul;52-54:413-425. doi: 10.1016/j.matbio.2016.02.002. Epub 2016 Feb 12. PMID: 26877077; PMCID: PMC4875828.

17. Shilling SH, Hjelmeland AB, Rich JN, Wang XF. TGF-β: multipotential cytokine. In: Derynck R, Miyazono K, eds. The TGF-β Family. New York: Cold Spring Harbor Laboratory Press, 2007: 49–77

18. A. Shoji-Matsunaga, T. Ono, M. Hayashi and H. Takayanagi, "Osteocyte regulation of orthodontic force-mediated tooth movement via RANKL expression," *Sci Rep,* vol. 7, no. 1, p. 8753, 2017.

19. Stemmler A, Symmank J, Steinmetz J, von Brandenstein K, Hennig CL, Jacobs C. "GDF15 Supports the Inflammatory Response of PdL Fibroblasts Stimulated by *P. gingivalis* LPS and Concurrent Compression." Int J Mol Sci. 2021

20. Takahashi N, Udagawa N, Suda T. A new member of tumor necrosis factor ligand family, ODF/OPGL/TRANCE/RANKL, regulates osteoclast differentiation and function. Biochem Biophys Res Commun. 1999 Mar 24;256(3):449-55. doi: 10.1006/bbrc.1999.0252. PMID: 10080918.

21. Tang SY, Alliston T. Regulation of postnatal bone homeostasis by TGFβ. Bonekey Rep. 2013 Jan 9;2:255. doi: 10.1038/bonekey.2012.255. PMID: 24404376; PMCID: PMC3722719.

22. Verborgt O, Gibson GJ, Schaffler MB. Loss of osteocyte integrity in association with microdamage and bone remodeling after fatigue in vivo. J Bone Miner Res. 2000 Jan;15(1):60-7. doi: 10.1359/jbmr.2000.15.1.60. PMID: 10646115.

23. Wada T, Nakashima T, Hiroshi N, Penninger JM. RANKL-RANK signaling in osteoclastogenesis and bone disease. Trends Mol Med. 2006 Jan;12(1):17-25. doi: 10.1016/j.molmed.2005.11.007. Epub 2005 Dec 13. PMID: 16356770.

24. S. Yadav, T. Dobie, A. Assefnia, H. Gupta and Z. Kalajzic, "Effect of low-frequency mechanical vibration on orthodontic tooth movement," *Am J Orthod Dentofacial Orthop,* vol. 148, no. 3, pp. 440-449, 2015.

25. C. Yang, H. Jeon, A. Alshabab, Y. Lee, C. Chung and D. Graves, "RANKL deletion in periodontal ligament and bone lining cells blocks orthodontic tooth movement," *International Journal of Oral Science,* vol. 10, no. 1, 2018.

Publishing Agreement

It is the policy of the University to encourage open access and broad distribution of all theses, dissertations, and manuscripts. The Graduate Division will facilitate the distribution of UCSF theses, dissertations, and manuscripts to the UCSF Library for open access and distribution. UCSF will make such theses, dissertations, and manuscripts accessible to the public and will take reasonable steps to preserve these works in perpetuity.

I hereby grant the non-exclusive, perpetual right to The Regents of the University of California to reproduce, publicly display, distribute, preserve, and publish copies of my thesis, dissertation, or manuscript in any form or media, now existing or later derived, including access online for teaching, research, and public service purposes.

DocuSigned by:
Albert Ngo
13E3CE762FBC4F0...
Author Signature

5/21/2023
Date